ANALYTICAL AND EXPERIMENTAL INVESTIGATION OF ALLEN AIRFOIL THEORY

A Thesis

Presented to

the Faculty of the Division of Graduate Studies

Georgia Institute of Technology

In Partial Fulfillment

of the Requirements for the Degree

Master of Science in Aeronautical Engineering

by

Allen Fordyce Latta

June 1950

Crossland

ANALYTICAL AND EXPERIMENTAL INVESTIGATION

OF ALLEN AIRFOIL THEORY

Approved:

Date Approved by Chairman June 28, 1950

ACKNOWLEDGMENTS

The author wishes to extend his sincere appreciation to Professor Alan Y. Pope for his valuable counsel and guidance in the execution of this thesis. Thanks are extended to Professor M. J. Goglia and to Professor H. W. S. Lavier for their review of this investigation. Also the writer is grateful for the help of Mr. W. C. Slocum in the construction of the model necessary to the program.

Appreciation is extended to the Faculty of the Daniel Guggenheim School of Aeronautics, Georgia Institute of Technology, for their help and suggestions.

PREFACE

SYMBOLS

A_o', A_o''	General coefficients in assumption of vorticity
A_n, B_n	General Fourier series coefficients
B_o', B_o''	General coefficients in assumption of base profile shape
C	Wing chord
C_l	Lift coefficient
L	Lift force
n	1, 2, 3, . . . ∞
p	Pressure
P	Pressure coefficient
${}_oP$	Pressure coefficient corresponding to zero airfoil thickness
P_b	Basic pressure coefficient distribution for airfoil of finite thickness
${}_oP_a$	Additional pressure coefficient distribution for airfoil of zero thickness
${}_oP_b$	Basic pressure coefficient distribution for airfoil of zero thickness
Q	Source or sink strength
q	Freestream dynamic pressure
r	Radius of airfoil leading edge
RN	Reynolds Number
RN_e	Effective Reynolds Number
T	Temperature ^oF
t	Airfoil thickness
T.F.	Wind tunnel turbulence factor
v	Local velocity

V	Velocity
V_o	Freestream velocity
V_i	Indicated freestream velocity
V_t	True freestream velocity
$\frac{V_f}{V_o}$	Base profile velocity distribution
$\frac{V_l}{V_o}$	Airfoil lower surface velocity distribution
$\frac{V_r}{V_o}$	Reference base profile velocity distribution
$\frac{V_u}{V_o}$	Airfoil upper surface velocity distribution
$\frac{\Delta v}{V_o}$	Base profile difference velocity distribution
x	Horizontal distance along chord; the abscissa of any point on the airfoil
x_l	Lower surface abscissa of any point on airfoil
x_u	Upper surface abscissa of any point on airfoil
y	Vertical distance perpendicular to chord; the ordinates of the airfoil
y_c	Ordinates of cambered airfoil
y_{c_b}	Ordinates of mean camber line corresponding to zero additional pressure distribution
y_t	Ordinates of airfoil base profile
y_u	Ordinates of cambered airfoil, upper surface
y_l	Ordinates of cambered airfoil, lower surface

α	Angle of attack
α_i	Ideal angle of attack
β	The angle whose tangent is $\frac{dy_c}{dx}$
${}_o\Gamma$	Vorticity for airfoil of zero thickness
Δ	Finite difference
θ	The angle whose cosine is $(1 - \frac{2c}{x})$
ρ	Mass density of air
μ	Viscosity of air

o	A subscript referring to any particular value of θ held constant during the process of integration

TABLE OF CONTENTS

LIST OF TABLES

LIST OF FIGURES

ANALYTICAL AND EXPERIMENTAL INVESTIGATION OF ALLEN AIRFOIL THEORY

SUMMARY

The Allen airfoil theory as given in Reference (1) is investigated analytically and experimentally with regard to the determination of the airfoil corresponding to a given velocity distribution.

The theory is carefully examined and much of the detailed information omitted in the above reference is presented.

Use of the theory is well illustrated and explained by assuming an arbitrary distribution of velocity from which the corresponding airfoil is computed by the method defined in Reference (1). A model of the derived airfoil was constructed and subsequently tested in the small, low speed wind tunnel at the Georgia Institute of Technology to obtain the actual velocity distribution over the profile.

The actual and the desired velocity distribution are compared with generally favorable results.

INTRODUCTION

The problem of determining the velocity distribution for an arbitrary airfoil, or the inverse problem of determining the airfoil for an arbitrary velocity distribution, has been solved mathematically by several investigators in recent years. Among the most notable of these theories is the work of Munk, Glauert, Theodorsen and Betz.

The method of Theodorsen in determining the velocity distribution corresponding to a given airfoil is particularly prominent, but it is not of utility in the solution of the inverse problem. A notable method of solving the inverse problem of determining the airfoil corresponding to an arbitrary velocity distribution is given by Betz in Reference (8), but this solution is intricate and laborious to apply.

Using the contributions of these and other researchers, an extension of the general theory involving certain new analysis has been developed by H. J. Allen at the Ames Aeronautical Laboratory of the National Advisory Committee for Aeronautics. The investigations by Allen have resulted in a new method presented in Reference (1) which solves either the direct or the inverse problem concerning airfoil shape and the corresponding velocity distribution. This method, which is comparatively rapid and easily applied, solves the problem directly and accurately.

The Allen solution results essentially from the fact that many of the properties of wing sections are primarily functions of the mean camber line or of the airfoil base profile. Thus, by the method defined in Reference (1), from an arbitrary velocity distribution the corresponding mean camber line and base profile are determined. Proper addition of these configurations then yields the airfoil corresponding to the arbitrary distribution of velocity. This is the problem considered and analyzed in this writing.

THEORY

The mean camber line theory and the base profile theory presented in Reference (1) are considered separately in detail in the subsequent pages. Equations are numbered in accordance with those of Reference (1) in order to facilitate comparison. The mean camber line is defined as the locus of points situated halfway between the upper and lower surfaces of the airfoil section, these distances being measured normal to the mean line. The base profile of the airfoil is the profile if the camber were removed and the resulting symmetrical airfoil set at zero angle of attack. Reference (9) shows that in a determination of the velocity distribution over a cambered airfoil the effects of the camber and the thickness distribution may be considered independently.

The analysis of the base profile is based upon the replacement of the actual base profile by a source-sink system, and similarly the mean camber line study evolves from replacing the mean line by a vortex system. The induced velocity at any point on the cambered airfoil, as demonstrated in Reference (9), may be found by superimposing the induced velocity at the point due to the vortex system and that at the point due to the source-sink system.

THE MEAN CAMBER LINE THEORY

Replace the actual mean camber line by an infinite number of point vortices employed along the same geometrical shape as the original camber line. Now, as shown in Figure A below, if the camber is small,

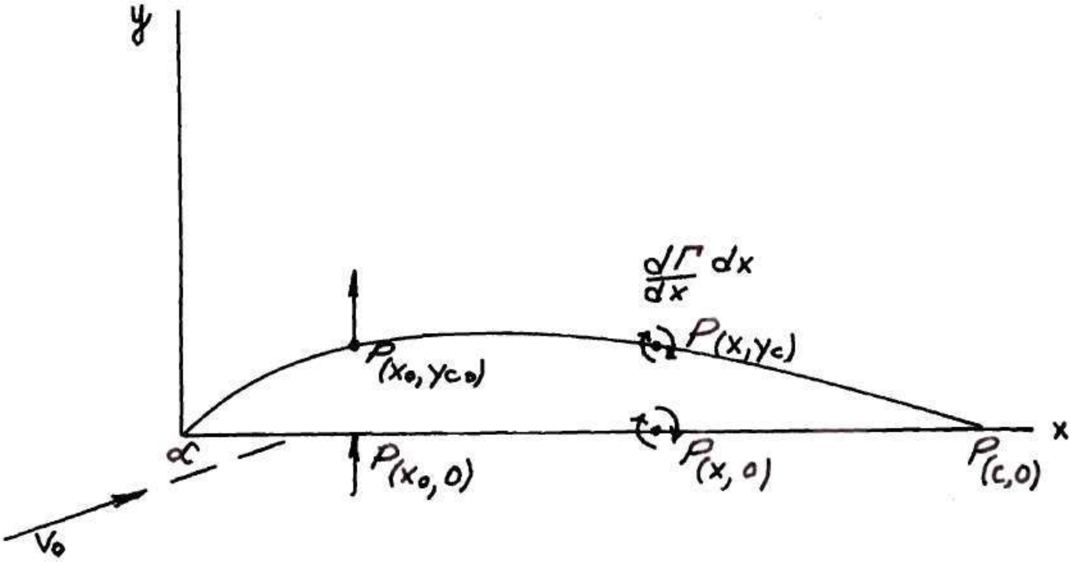

Figure A, Diagram of mean camber line

the velocity induced at a point $P(x_o, y_{co})$ on the mean camber line by a vortex at any other point $P(x, y_c)$ on this line is approximately that which would be induced at the point on the x axis $P(x_o, 0)$ by the same vortex at the point $P(x, 0)$. $\Gamma_t = \int_0^c \Gamma dx$ and the vortex strength at any point is $\frac{d\Gamma}{dx}dx$. The velocity induced at any point on the camber line due to all the vortices distributed along the camber line is

$$v_{(x_o)} = \frac{1}{2\pi}\int_0^c \frac{\frac{d\Gamma}{dx}dx}{(x - x_o)} \tag{1}$$

as shown in Reference (2), and is perpendicular to the x-axis. The flow direction close to the camber line must be parallel to the surface of the camber line so that if the angle α between the x-axis and the direction of flow of the undisturbed stream is small, then it is evident from Figure B that

$$\frac{v}{V_o} = \frac{dy_c}{dx} - \alpha \qquad (2)$$

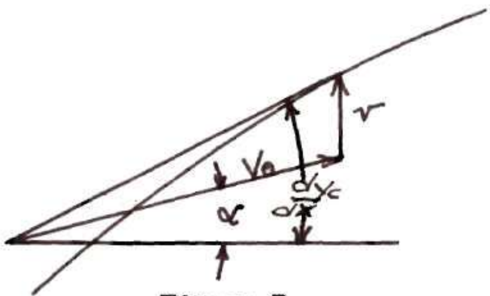

Figure B

where Vo is the velocity of the undisturbed stream.

At this point it is convenient to introduce the new coordinate θ such that

$$\begin{aligned} x &= c/2(1 - \cos\theta) \\ x_o &= c/2(1 - \cos\theta_o) \\ dx &= c/2 \sin\theta \, d\theta \end{aligned} \qquad (3)$$

where c is the airfoil chord. Assuming the distribution of vorticity ${}_o\Gamma$, where the prescript $_o$ indicates that this circulation applies to an airfoil of zero thickness, along the x-axis to be:

$$\frac{d\,{}_o\Gamma}{dx} = 2V_o\left[A_o' \cot\theta/2 + A_o'' \tan\theta/2 + \sum_1^{\infty} A_n \sin n\theta\right] \qquad (4)$$

Then

$$\frac{d\,{}_o\Gamma}{dx}dx = 2V_o\frac{c}{2}\left[A_o'\sqrt{\frac{1+\cos\theta}{1-\cos\theta}}\sqrt{(1-\cos\theta)(1+\cos\theta)}\right.$$

$$\left. + A_o''\sqrt{\frac{1-\cos\theta}{1+\cos\theta}}\sqrt{(1-\cos\theta)(1+\cos\theta)} + \sum_1^{\infty} A_n \sin\theta \sin n\theta\right]d\theta$$

and

$$\frac{d_o\Gamma\, dx}{dx} = cV_o\left\{A_o'(1+\operatorname{Cos}\theta) + A_o''(1-\operatorname{Cos}\theta) + \sum_1^{\infty} A_n \operatorname{Sin} n\theta \operatorname{Sin}\theta\right\}d\theta \quad (5)$$

And now from equations (1), (2), (3), and (5), the slope at θ_o may be obtained as follows: Substitute equation (5) into equation (1) and we have

$$v(x_o) = \frac{1}{2\pi}\int_0^{\pi}\frac{cV_o\left\{A_o'(1+\operatorname{Cos}\theta) + A_o''(1-\operatorname{Cos}\theta) + \sum_1^{\infty} A_n\operatorname{Sin} n\theta\operatorname{Sin}\theta\right\}d\theta}{\frac{c}{2}(1-\operatorname{Cos}\theta) - \frac{c}{2}(1-\operatorname{Cos}\theta_o)}$$

hence

$$\frac{dy_{c_o}}{dx} - \alpha = \frac{v}{V_o} = \frac{cV_o}{2\pi V_o}\int_0^{\pi}\frac{\left\{A_o'(1+\operatorname{Cos}\theta) + A_o''(1-\operatorname{Cos}\theta) + \sum_1^{\infty} A_n\operatorname{Sin} n\theta\operatorname{Sin}\theta\right\}d\theta}{c/2\ (\operatorname{Cos}\theta_o - \operatorname{Cos}\theta) + c/2 - c/2}$$

Now from the trignometric identity Sin A Sin B $= \frac{1}{2}\left\{\operatorname{Cos}(A-B) - \operatorname{Cos}(A+B)\right\}$, we may write Sin $n\theta$ Sin θ $= \frac{1}{2}\left\{\operatorname{Cos}(n-1)\theta - \operatorname{Cos}(n+1)\theta\right\}$ and thus

$$\frac{dy_{c_o}}{dx} - \alpha = \frac{1}{\pi}\int_0^{\pi}\frac{\left[A_o'(1+\operatorname{Cos}\theta) + A_o''(1-\operatorname{Cos}\theta) + \frac{1}{2}\sum_1^{\infty} A_n\left\{\operatorname{Cos}(n-1)\theta - \operatorname{Cos}(n+1)\theta\right\}\right]d\theta}{\operatorname{Cos}\theta_o - \operatorname{Cos}\theta} \quad (6)$$

It is shown in Reference (2) that

$$\int_0^{\pi}\frac{\operatorname{Cos} n\theta\, d\theta}{\operatorname{Cos}\theta - \operatorname{Cos}\theta_o} = \frac{\pi\operatorname{Sin} n\theta_o}{\operatorname{Sin}\theta_o}$$

or

$$\int_0^{\pi}\frac{\operatorname{Cos} n\theta\, d\theta}{\operatorname{Cos}\theta_o - \operatorname{Cos}\theta} = \frac{-\pi\operatorname{Sin} n\theta_o}{\operatorname{Sin}\theta_o} \quad (7)$$

and now equation (6) may be written in this particular form as follows:

$$\frac{dy_c}{dx} - \alpha = \frac{1}{\pi}\int_0^{\pi}\frac{\left\{(A_0'+A_0'')\cos 0\theta + (A_0'-A_0'')\cos\theta + \frac{1}{2}\sum_1^{\infty} A_n\left[\cos(n-1)\theta - \cos(n+1)\theta\right]\right\}d\theta}{\cos\theta_0 - \cos\theta}$$

Therefore, equation (7) yields:

$$\frac{dy_c}{dx} - \alpha = \frac{1}{\pi}(A_0'+A_0'')\frac{(-\pi\sin 0\theta_0)}{\sin\theta_0} + \frac{1}{\pi}(A_0'-A_0'')\frac{(-\pi\sin\theta_0)}{\sin\theta_0}$$

$$+ (1/2\pi)\sum_1^{\infty} A_n\left[\frac{-\pi\sin(n-1)\theta_0 + \pi\sin(n+1)\theta_0}{\sin\theta_0}\right]$$

Using the trignometric identity, $\sin A - \sin B = 2\cos\left[\frac{(A+B)}{2}\right]\sin\left[\frac{(A-B)}{2}\right]$,

we have:

$$\sin(n+1)\theta_0 - \sin(n-1)\theta_0 = 2\cos\left[\frac{(n+1+n-1)\theta_0}{2}\right]\sin\left[\frac{(n+1-n+1)\theta_0}{2}\right]$$

$$= 2\cos n\theta_0 \sin\theta_0$$

so that:

$$\frac{dy_c}{dx} = \alpha - A_0' + A_0'' + \frac{1}{2}\,2\sum_1^{\infty}\frac{A_n\cos n\theta_0\sin\theta_0}{\sin\theta_0}$$

and finally

$$\frac{dy_c}{dx} = \alpha - A_0' + A_0'' + \sum_1^{\infty} A_n\cos n\theta_0 \qquad (8)$$

and now integrating from 0 to π,

$$\int_0^{\pi}\frac{dy_c}{dx}\cdot d\theta = \int_0^{\pi}(\alpha - A_0' + A_0'')\,d\theta + \sum_1^{\infty}\int_0^{\pi} A_n\left(\cos n\theta\right)d\theta$$

$$\int_0^{\pi} \frac{dy_c}{dx} \cdot d\theta = \pi(\alpha - A_o' + A_o'') + \sum_1^{\infty} \frac{A_n}{n} \operatorname{Sin} n\theta \Big]_0^{\pi}$$

hence, since the last term vanishes for all n, the coefficients are given by

$$\alpha - A_o' + A_o'' = \frac{1}{\pi} \int_0^{\pi} \frac{dy_c}{dx} \cdot d\theta \qquad (9a)$$

The general coefficient, A_n, is found as follows: multiplying equation (8) by Cos $n\theta$, we have by integrating:

$$\int_0^{\pi} \frac{dy_c}{dx} \operatorname{Cos} n\theta \, d\theta = \int_0^{\pi} (\alpha - A_o' + A_o'') \operatorname{Cos} n\theta \, d\theta + A_n \int_0^{\pi} \operatorname{Cos}^2(n\theta) \, d\theta,$$ since

all of the cosine terms in the summation vanish upon integration from 0 to π except the $\operatorname{Cos}^2(n\theta)$ term. And now performing the indicated integration:

$$\int_0^{\pi} \frac{dy_c}{dx} \operatorname{Cos} n\theta \, d\theta = \frac{1}{n}(\alpha - A_o' + A_o'') \operatorname{Sin} n\theta \Big]_0^{\pi} + A_n/2 \left[\left(\theta + \frac{\operatorname{Sin} 2n\theta}{2n}\right)\right]_0^{\pi}$$

$$\int_0^{\pi} \frac{dy_c}{dx} \operatorname{Cos} n\theta \, d\theta = \frac{\pi}{2} A_n,$$ and thus we write

$$A_n = \frac{2}{\pi} \int_0^{\pi} \frac{dy_c}{dx} \operatorname{Cos} n\theta \, d\theta \qquad (9b)$$

The lift force may be found from

$${}_oL = \int_0^{c} \rho V_o \frac{d({}_o\Gamma)dx}{dx},$$ and substituting equation (5) for $\frac{d\, {}_o\Gamma dx}{dx}$

$$ {}_oL = \rho(V_o)^2 c \int_0^{\pi} \left[A_o'(1+\cos\theta) + A_o''(1-\cos\theta) + \sum_1^{\infty} A_n \sin n\theta \sin\theta \right] \cdot d\theta $$

$$ {}_oL = \rho(V_o)^2 c \int_0^{\pi} (A_o' + A_o'')d\theta + \rho c(V_o)^2 \int_0^{\pi} (A_o' - A_o'') \cos\theta \, d\theta $$

$$ + \rho c(V_o)^2 \sum_1^{\infty} A_n \int_0^{\pi} \left[\cos(n-1)\theta - \cos(n+1)\theta \right] d\theta $$

Upon performing the integration, we have

$$ {}_oL = \rho c(V_o)^2 (A_o' + A_o'')\pi + \rho c(V_o)^2 (A_o' - A_o'') (\sin\pi - \sin 0) $$

$$ + \rho \frac{c(V_o)^2}{2} \sum_1^{\infty} A_n \left[\frac{\sin(n-1)\theta}{(n-1)} - \frac{\sin(n+1)\theta}{(n+1)} \right]_0^{\pi} $$

The last term of the above expression vanishes for all values of "n" except for n = 1 for which $\frac{\sin(n-1)\theta}{(n-1)}$ is indeterminate in its present form. Therefore:

$$ {}_oL = \rho c(V_o)^2 \pi (A_o' + A_o'') + \rho \frac{c(V_o)^2}{2} \cdot \left[A_1 \frac{\sin(n-1)\pi}{(n-1)} \right] $$

Consider the last term: expanding and dividing by (n - 1) yields:

$$ \frac{\sin(n-1)\pi}{(n-1)} = \frac{(n-1)\pi}{(n-1)} - \frac{(n-1)^3\pi^3}{(n-1)\,\lfloor 3} + \frac{(n-1)^5\pi^5}{(n-1)\,\lfloor 5} - \frac{(n-1)^7\pi^7}{(n-1)\,\lfloor 7} \cdots\cdots $$

$$ \frac{\sin(n-1)\pi}{(n-1)} = \pi - \frac{(n-1)^2\pi^3}{\lfloor 3} + \frac{(n-1)^4\pi^5}{\lfloor 5} - \frac{(n-1)^6\pi^7}{\lfloor 7} + \frac{(n-1)^8\pi^9}{\lfloor 9} \cdots $$

For n = 1, the value of $\frac{\sin(n-1)\pi}{(n-1)}$ becomes π.

Hence: ${}_oL = \rho c(V_o)^2 \pi (A_o' + A_o'' + \frac{1}{2} A_1)$

so that the lift coefficient is,

$$ {}_oC_l = 2\pi (A_o' + A_o'' + \frac{1}{2} A_1) \tag{10} $$

In the case of an airfoil wherein the trailing edge is sharp, the "Kutta condition" must be satisfied. This condition is that enough circulation will arise about the airfoil so that the flow will leave the trailing edge smoothly. This hypothesis, in turn, requires that there shall be no angular velocity, ω , at the airfoil trailing edge. Hence the vorticity is zero at the trailing edge, and this condition requires that the $A_o'' = 0$. The coefficients therefore become

$$ \begin{aligned} A_o' &= \alpha - \frac{1}{\pi}\int_o^{\pi} \frac{dy_c}{dx}\, d\theta \\ A_o'' &= 0 \\ A_n &= \frac{2}{\pi}\int_o^{\pi} \frac{dy_c}{dx} \operatorname{Cos} n\theta \, d\theta \end{aligned} \tag{13} $$

It is noted in Reference (2) that the coefficients A_n of the Sin $n\theta$ series in the assumed distribution of vorticity of equation (4) are independent of the angle of attack and are functions of the mean camber-line shape only. The coefficient A_o' varies with the angle of attack.

Now the pressure coefficient P is expressed in terms of q, the stream dynamic pressure. ${}_oP$ is the difference at x between the upper and lower surface pressure coefficients, $P_l - P_u$; and hence from the Kutta-Joukowski theorem of lift,

$$ {}_oP = \frac{\rho V_o \frac{d({}_o\Gamma)}{dx}}{q} = \frac{\rho V_o \frac{d({}_o\Gamma)}{dx}}{(\rho/2)(V_o)^2} = \frac{2}{V_o}\,\frac{d({}_o\Gamma)}{dx} \tag{14} $$

and now substituting from equation (4)

$$ {}_oP = \frac{2}{V_o} \; 2\,V_o \left(A_o' \,\mathrm{Cot}\, \frac{1}{2}\theta + A_o'' \,\mathrm{Tan}\, \frac{1}{2}\theta + \sum_1^{\infty} A_n \,\mathrm{Sin}\, n\theta \right) \tag{15} $$

It has been found convenient in the past to consider the above expression for the chordwise pressure distribution to be composed of two distinct parts. This concept first appeared in Reference (3). That part which is in magnitude independent of the angle of attack and in form dependent solely upon the camberline shape is known as the basic pressure distribution, and that which is in magnitude variable with the angle of attack and in form independent of the mean camber-line shape is the additional pressure distribution. Hence, for the infinitesimally thin airfoil the additional pressure distribution is given by

$$ {}_oP_a = 4(A_o' \,\mathrm{Cot}\, \frac{1}{2}\theta), \text{ since } A_o'' = 0, \tag{16} $$

and the basic pressure distribution is given by

$$ {}_oP_b = 4 \sum_1^{\infty} A_n \,\mathrm{Sin}\, n\theta \tag{17} $$

It is convenient to consider the basic lift distribution only as characteristic of a given camber-line shape since the additional distribution may be modified at will by a change in the angle of attack and so, at some angle, must be zero. The angle of attack at which the magnitude of the additional distribution is zero for an airfoil is known as the "ideal angle, α_i". For an airfoil for which the Kutta condition holds, the magnitude of the additional distribution is determined by the coefficient A_o', which is given as the first of equations (13) as

$$ A_o' = \alpha - \frac{1}{\pi} \int_0^{\pi} \frac{dy_c}{dx} \, d\theta $$

Since when $\alpha = \alpha_i$, $A_0' = 0$, then we have that the ideal angle α_i is

$$\alpha_i = \frac{1}{\pi}\int_0^{\pi} \frac{dy_c}{dx}\, d\theta \tag{18}$$

The ordinates of the mean camber line corresponding to the case when the additional distribution is zero, denoted by y_{c_b}, are related to the ordinates y_c as shown in Figure C below.

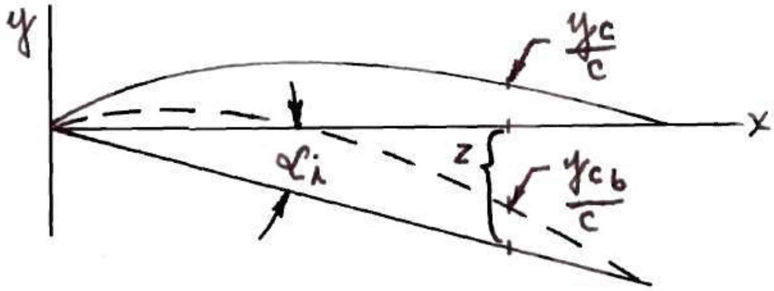

Figure C

The magnitude of α_i is inherently very small. Figure C has shown α_i greatly enlarged to clarify the sketch. The following relations are derived considering α_i to be very small.

$$\operatorname{Tan} \alpha_i = \frac{z}{x/c} = \alpha_i \,. \quad \text{Thus,} \quad \frac{y_{c_b}}{c} = \frac{y_c}{c} - \frac{x}{c}\alpha_i \tag{19}$$

and differentiation yields

$$\frac{dy_{c_b}}{dx} = \frac{dy_c}{dx} - \alpha_i \tag{20}$$

Now substituting equation (8) into equation (20) gives: since $\alpha = \alpha_i$, $A_0'' = 0$, and considering only the basic distribution since the additional distribution is zero at α_i

$$\frac{dy_{cb}}{dx} = \alpha_i - 0 + 0 + \sum_1^\infty A_n \cos n\theta \quad - \alpha_i$$

$$\frac{dy_{cb}}{dx} = \sum_1^\infty A_n \cos n\theta \tag{20a}$$

Thus we have from equations (17) and (20a) the following two series:

$$\begin{aligned} \frac{dy_{cb}}{dx} &= \sum_1^\infty A_n \cos n\theta \\ \frac{{}_oP_b}{4} &= \sum_1^\infty A_n \sin n\theta \end{aligned} \tag{21}$$

The coefficients A_n of these equations are developed as follows:

Consider $\frac{dy_{cb}}{dx} = \sum_1^\infty A_n \cos n\theta$. Multiply the equation by Cos $n\theta$ and integrate from 0 to π. Thus

$\int_0^\pi \frac{dy_{cb}}{dx} \cos n\theta \, d\theta = A_n \int_0^\pi \cos^2 (n\theta) \, d\theta$ since all of the Cosine products disappear upon integration from 0 to π except $\cos^2(n\theta)$.

Hence

$$\int_0^\pi \frac{dy_{cb}}{dx} \cos n\theta \, d\theta = \frac{A_n}{2} \left[\theta + \frac{\sin 2n\theta}{2\,n} \right]_0^\pi$$

and

$$\int_0^\pi \frac{dy_{cb}}{dx} \cos n\theta \, d\theta = \frac{\pi A_n}{2}$$

Therefore

$$A_n = \frac{2}{\pi} \int_0^\pi \frac{dy_{cb}}{dx} \cos n\theta \, d\theta \tag{22a}$$

In a similar manner, consider the series $\frac{{}_oP_b}{4} = \sum_1^\infty A_n \sin n\theta$. Multiply by Sin $n\theta$ and integrate from 0 to π. Thus

$$\int_0^{\pi} \frac{{}_oP_b}{4} \text{Sin } n\theta \, d\theta = A_n \int_0^{\pi} \text{Sin}^2 (n\theta) \, d\theta$$ since all the Sine

products disappear upon integration from 0 to π except $\text{Sin}^2 (n\theta)$. Hence

$$\int_0^{\pi} \frac{{}_oP_b}{4} \text{Sin } n\theta \, d\theta = \frac{A_n}{2} \left[\theta - \frac{\text{Sin } 2n\theta}{2\,n}\right]_0^{\pi}$$

and

$$\int_0^{\pi} \frac{{}_oP_b}{4} \text{Sin } n\theta \, d\theta = \frac{\pi A_n}{2}$$

Therefore

$$A_n = \frac{2}{\pi} \int_0^{\pi} \frac{{}_oP_b}{4} \text{Sin } n\theta \, d\theta \qquad (22b)$$

Using equations (21) and (22), the chordwise pressure distribution corresponding to a given mean camber line or the mean camber line corresponding to a given chordwise pressure distribution can be found. However, in general the calculations using the above infinite series will be very lengthy so that it is desirable to replace the Fourier expansions by integral expressions, as was done in the development of the method of Reference (4). In order to accomplish this, the expression for the Fourier coefficients given by the equations (22) can be substituted in equations (21). At the point θ_o then

$$\frac{{}_oP_{b_o}}{4} = \frac{2}{\pi} \int_0^{\pi} \frac{dy_{c_b}}{dx} \sum_1^{\infty} \text{Sin } n\theta_o \text{ Cos } n\theta \, d\theta \qquad (23a)$$

and
$$\frac{dy_{cb_o}}{dx} = \frac{2}{\pi}\int_0^{\pi} \frac{{}_oP_b}{4} \sum_1^{\infty} \operatorname{Sin} n\theta \operatorname{Cos} n\theta_o \, d\theta \tag{23b}$$

It is to be noted that the interchanging of the integral sign, $\int$, and the summation sign, $\sum$, necessary in the obtaining of equations (23) is actually an assumption of uniform convergence of the function. Theodorsen, in Reference (4) where this procedure first appears, has considered a basic transformation which he defines as composed of uniformly convergent series. Since equations (23) result from manipulation of these particular series, no further qualification of equations (23) is given. θ_o simply indicates the angle kept constant while the integrations are performed.

Now,

$$\begin{aligned} \operatorname{Sin} n\theta_o \operatorname{Cos} n\theta &= \frac{1}{2}\left[\operatorname{Sin} n(\theta+\theta_o) - \operatorname{Sin} n(\theta-\theta_o)\right] \\ \operatorname{Sin} n\theta \operatorname{Cos} n\theta_o &= \frac{1}{2}\left[\operatorname{Sin} n(\theta+\theta_o) + \operatorname{Sin} n(\theta-\theta_o)\right] \end{aligned} \tag{23c}$$

and further, it is given in References (4) and (5) that

$$\sum_1^{n} \operatorname{Sin} n(\theta \pm \theta_o) = \frac{1}{2}\operatorname{Cot}\left(\frac{\theta \pm \theta_o}{2}\right) - \frac{\operatorname{Cos}\,(2n+1)\left(\frac{\theta \pm \theta_o}{2}\right)}{2\operatorname{Sin}\left(\frac{\theta \pm \theta_o}{2}\right)} \tag{23d}$$

so that substitution of (23c) into equations (23a) and (23b) gives

$$\frac{{}_oP_{b_o}}{4} = \frac{2}{\pi}\int_0^{\pi} \frac{dy_{cb}}{dx} \sum_1^{\infty} \frac{1}{2}\left[\operatorname{Sin} n(\theta+\theta_o) - \operatorname{Sin} n(\theta-\theta_o)\right] d\theta$$

$$\frac{dy_{cb_o}}{dx} = \frac{2}{\pi}\int_0^{\pi} \frac{{}_oP_b}{4} \sum_1^{\infty} \frac{1}{2}\left[\operatorname{Sin} n(\theta+\theta_o) + \operatorname{Sin} n(\theta-\theta_o)\right] d\theta$$

and now substituting equation (23d) into the above expressions

$$\frac{{}_oP_{b_o}}{4} = \lim_{n\to\infty}\left\{\frac{1}{2\pi}\int_0^{\pi}\frac{dy_{cb}}{dx}\left[\mathrm{Cot}\left(\frac{\theta+\theta_o}{2}\right) - \mathrm{Cot}\left(\frac{\theta-\theta_o}{2}\right)\right]d\theta\right.$$

$$\left. - \frac{1}{2\pi}\int_0^{\pi}\frac{dy_{cb}}{dx}\left[\frac{\mathrm{Cos}(2n+1)\left(\frac{\theta+\theta_o}{2}\right)}{\mathrm{Sin}\left(\frac{\theta+\theta_o}{2}\right)} - \frac{\mathrm{Cos}(2n+1)\left(\frac{\theta-\theta_o}{2}\right)}{\mathrm{Sin}\left(\frac{\theta-\theta_o}{2}\right)}\right]d\theta\right\} \quad (23e)$$

and similarly

$$\frac{dy_{cb_o}}{dx} = \lim_{n\to\infty}\left\{\frac{1}{2\pi}\int_0^{\pi}\frac{{}_oP_b}{4}\left[\mathrm{Cot}\left(\frac{\theta+\theta_o}{2}\right) + \mathrm{Cot}\left(\frac{\theta-\theta_o}{2}\right)\right]d\theta\right.$$

$$\left. - \frac{1}{2\pi}\int_0^{\pi}\frac{{}_oP_b}{4}\left[\frac{\mathrm{Cos}\ (2n+1)\left(\frac{\theta+\theta_o}{2}\right)}{\mathrm{Sin}\left(\frac{\theta+\theta_o}{2}\right)} + \frac{\mathrm{Cos}\ (2n+1)\left(\frac{\theta-\theta_o}{2}\right)}{\mathrm{Sin}\left(\frac{\theta-\theta_o}{2}\right)}\right]d\theta\right\} (23f)$$

Now consider the second integrals in the above expressions for $\frac{{}_oP_{b_o}}{4}$ and $\frac{dy_{cb_o}}{dx}$. First let us examine the second integral in the equation for $\frac{{}_oP_{b_o}}{4}$. It is noted that the slope of the camber-line, $\frac{dy_{cb}}{dx}$, is uniquely determined at the point θ_o about which the integration is being performed, and hence is constant for any particular integration. Note that the values of n as defined in equations (21) range from 1 to ∞. At this point a special condition is imposed upon θ_o, and this is that $0 < \theta_o < \pi$. The method presented here is to prove that the second integrals vanish for all values of $0 < \theta_o < \pi$; and then to consider the special cases where $\theta_o = 0$ and π. The second integral in the equation for $\frac{{}_oP_b}{4}$ is

$$I = \lim_{n\to\infty}\int_0^{\pi} \frac{1}{2\pi}\frac{dy_{cb}}{dx}\left[\frac{\cos(2n+1)\left(\frac{\theta+\theta_o}{2}\right)}{\sin\left(\frac{\theta+\theta_o}{2}\right)} - \frac{\cos(2n+1)\left(\frac{\theta-\theta_o}{2}\right)}{\sin\left(\frac{\theta-\theta_o}{2}\right)}\right] d\theta$$

Now for simplification of the symbols we define: $\frac{dy_{cb}}{dx} = C$; $(2n + 1) = k$. Also, in the first term above we put $\left(\frac{\theta + \theta_o}{2}\right) = x$. Therefore, $d\theta = 2\,dx$; $\theta = \pi$ gives $x = \pi/2 + \theta_o/2$; $\theta = 0$ gives $x = \theta_o/2$. Likewise, put $\left(\frac{\theta - \theta_o}{2}\right) = x$ in the second term. This is valid since the integration is between limits and the variable disappears when the limits are substituted. Hence for the second integral: $d\theta = 2dx$; $\theta = \pi$ gives $x = \pi/2 - \theta_o/2$; $\theta = 0$ gives $x = -\theta_o/2$.

Substituting we have

$$I = \frac{2C}{2\pi}\int_{\frac{\theta_o}{2}}^{\frac{\pi}{2}+\frac{\theta_o}{2}} \frac{\cos kx\,dx}{\sin x} - \frac{2C}{2\pi}\int_{-\frac{\theta_o}{2}}^{\frac{\pi}{2}-\frac{\theta_o}{2}} \frac{\cos kx\,dx}{\sin x}$$

Dividing by $\frac{C}{\pi}$, then adding and subtracting $\int_{\frac{\pi}{2}-\frac{\theta_o}{2}}^{\frac{\theta_o}{2}} \frac{\cos kx\,dx}{\sin x}$, we have

$$\frac{I}{C/\pi} = \int_{\pi/2-\theta_o/2}^{\theta_o/2} \frac{\cos kx\,dx}{\sin x} + \int_{\theta_o/2}^{\pi/2+\theta_o/2} \frac{\cos kx\,dx}{\sin x} - \int_{-\theta_o/2}^{\pi/2-\theta_o/2} \frac{\cos kx\,dx}{\sin x} - \int_{\pi/2-\theta_o/2}^{\theta_o/2} \frac{\cos kx\,dx}{\sin x}$$

Therefore,

$$\frac{I}{C/\pi} = \int_{\pi/2-\theta_o/2}^{\pi/2+\theta_o/2} \frac{\cos kx\,dx}{\sin x} - \int_{-\theta_o/2}^{+\theta_o/2} \frac{\cos kx\,dx}{\sin x} \qquad (23g)$$

Consider now the first integral, and apply integration by parts. Let $\text{Cos } kx\, dx = dv$; hence $v = \frac{\text{Sin } kx}{k}$. Let $u = \frac{1}{\text{Sin } x}$; hence $du = -\frac{\text{Cos } x\, dx}{\text{Sin}^2 x}$ and thus

$$\int_{\pi/2-\theta_o/2}^{\pi/2+\theta_o/2} \frac{\text{Cos } kx\, dx}{\text{Sin } x} = \left.\frac{\text{Sin } kx}{k \text{ Sin } x}\right]_{\pi/2-\theta_o/2}^{\pi/2+\theta_o/2} + \frac{1}{k} \times \int_{\pi/2-\theta_o/2}^{\pi/2+\theta_o/2} \frac{\text{Sin } kx \text{ Cos } x\, dx}{\text{Sin}^2 x} .$$

Since the Sine terms are always of such a magnitude that the expressions in the brackets and under the integral sign are finite within the above ranges of integration, these expressions vanish as $k \to \infty$. Thus

$$\lim_{k\to\infty} \int_{\pi/2-\theta_o/2}^{\pi/2+\theta_o/2} \frac{\text{Cos } kx\, dx}{\text{Sin } x} \to 0$$

Now consider the second integral, $\int_{-\theta_o/2}^{\theta_o/2} \frac{\text{Cos } kx\, dx}{\text{Sin } x}$ Since $\text{Sin } x = 0$ within the range of integration, the function is not continuous. Therefore, we write the integral in the standard form for evaluating an integral which is discontinuous at a point:

$$\int_{-\theta_o/2}^{\theta_o/2} \frac{\text{Cos } kx\, dx}{\text{Sin } x} = \lim_{\epsilon\to 0} \left[+ \int_{-\theta_o/2}^{0-\epsilon} \frac{\text{Cos } kx\, dx}{\text{Sin } x} + \int_{0+\epsilon}^{\theta_o/2} \frac{\text{Cos } kx\, dx}{\text{Sin } x} \right] .$$

In the first integral term above, let $x = -x$; thus $dx = -dx$. When

$x = -\epsilon$, $-x = +\epsilon$; when $x = -\theta_o/2$, $-x = +\theta_o/2$. Substituting and writing the second integral first

$$\int_{-\theta_o/2}^{\theta_o/2} \frac{\cos kx\,dx}{\sin x} = \lim_{\epsilon \to 0}\left[\int_{\epsilon}^{\theta_o/2} \frac{\cos kx\,dx}{\sin x} + \int_{\theta_o/2}^{\epsilon} \frac{\cos kx\,dx}{\sin x}\right]$$

$$\text{Thus} \int_{-\theta_o/2}^{\theta_o/2} \frac{\cos kx\,dx}{\sin x} = \lim_{\epsilon \to 0} \int_{\epsilon}^{\epsilon} \frac{\cos kx\,dx}{\sin x} = \int_{0}^{0} \frac{\cos kx\,dx}{\sin x} = 0 \qquad (23h)$$

Therefore

$$I = \lim_{n \to \infty} \int_0^{\pi} \frac{1}{2\pi} \frac{dy_{c_b}}{dx} \left[\frac{\cos\,(2n+1)\left(\frac{\theta + \theta_o}{2}\right)}{\sin\left(\frac{\theta + \theta_o}{2}\right)} - \frac{\cos\,(2n+1)\left(\frac{\theta - \theta_o}{2}\right)}{\sin\left(\frac{\theta - \theta_o}{2}\right)} \right] d\theta = 0$$

And now turning to a similar examination of the second integral in the expression for $\frac{dy_{cb_o}}{dx}$, we observe the following conditions: the value of the basic pressure distribution, $\frac{{}_oP_b}{4}$, is uniquely determined at the point θ_o about which the integration is being performed, and hence is constant for any particular integration. $1 \leq n \leq \infty$; $0 < \theta_o < \pi$. As was noted previously the method presented here is to prove that the second integrals vanish for all values of $0 < \theta_o < \pi$; and then to consider the special cases where $\theta_o = 0$ and π. The second integral in the equation for $\frac{dy_{cb_o}}{dx}$ is

$$I = \lim_{n\to\infty} \int_0^{\pi} \frac{1}{2\pi}\,\frac{{}_oP_b}{4}\left[\frac{\cos\,(2n+1)\left(\frac{\theta+\theta_o}{2}\right)}{\sin\left(\frac{\theta+\theta}{2}\right)} + \frac{\cos\,(2n+1)\left(\frac{\theta-\theta_o}{2}\right)}{\sin\left(\frac{\theta-\theta_o}{2}\right)}\right] d\theta$$

Now as before, for simplification of the symbols, we define: $\frac{{}_oP_b}{4} = C$; $(2n+1) = k$. Also, in the first term above we put $\frac{\theta+\theta_o}{2} = x$; therefore, $d\theta = 2dx$, $\theta = \pi$ gives $x = \pi/2 + \theta_o/2$, $\theta = 0$ gives $x = \theta_o/2$. And likewise, put $\frac{\theta-\theta_o}{2} = x$ in the second term, as previously explained. Hence $d\theta = 2\,dx$; $\theta = \pi$ gives $x = \pi/2 - \theta_o/2$; $\theta = 0$ gives $x = -\theta_o/2$. Substituting we have

$$I = \lim_{k\to\infty}\left[\frac{C}{\pi}\int_{\theta_o/2}^{\pi/2+\theta_o/2}\frac{\cos kx\,dx}{\sin x} + \frac{C}{\pi}\int_{-\theta_o/2}^{\pi/2-\theta_o/2}\frac{\cos kx\,dx}{\sin x}\right]$$

Dividing by C/π and rewriting, we have as follows:

$$\frac{I}{C/\pi} = \lim_{k\to\infty}\left[\int_{\theta_o/2}^{\pi/2+\theta_o/2}\frac{\cos kx\,dx}{\sin x} + \int_{-\theta_o/2}^{\theta_o/2}\frac{\cos kx\,dx}{\sin x} + \int_{\theta_o/2}^{\pi/2-\theta_o/2}\frac{\cos kx\,dx}{\sin x}\right]$$

Now as previously shown the integral $\int_{-\theta_o/2}^{\theta_o/2}\frac{\cos kx\,dx}{\sin x} = 0$, and applying integration by parts to the first and third integrals, we have

$$\frac{I}{C/\pi} = \lim_{k\to\infty}\left\{ \left.\frac{\sin kx}{k \sin x}\right]_{\theta_o/2}^{\pi/2+\theta_o/2} + \int_{\theta_o/2}^{\pi/2+\theta_o/2}\frac{\sin kx \cos x\,dx}{k\,\sin^2 x} + \left.\frac{\sin kx}{k\sin x}\right]_{\theta_o/2}^{\pi/2-\theta_o/2} + \right.$$

$$+ \int_{\theta_o/2}^{\pi/2 - \theta_o/2} \frac{\text{Sin } kx \text{ Cos } x \, dx}{k \text{ Sin}^2 x} \Bigg\}$$

Since the Sine terms are always of such a magnitude that the expressions in the brackets and under the integral sign are always finite within the above ranges of integration, these expressions vanish as $k \longrightarrow \infty$.

Therefore

$$I = \lim_{n \to \infty} \frac{1}{2\pi} \int_0^{\pi} \frac{{}_oP_b}{4} \left[\frac{\text{Cos}(2n+1)\left(\frac{\theta + \theta_o}{2}\right)}{\text{Sin}\left(\frac{\theta + \theta_o}{2}\right)} + \frac{\text{Cos}(2n+1)\left(\frac{\theta - \theta_o}{2}\right)}{\text{Sin}\left(\frac{\theta - \theta_o}{2}\right)} \right] d\theta = 0 .$$

And thus it has been demonstrated that the second integrals in the expressions for $\frac{{}_oP_{b_o}}{4}$, equation (23e); and $\frac{dy_{cb_o}}{dx}$, equation (23f) vanish as $n \to \infty$, $0 < \theta_o < \pi$.

Consider now the special case where $\theta_o = \pi$; that is, at the trailing edge. Examination of equation (21) reveals that $\frac{{}_oP_b}{4} = 0$ at $\theta_o = \pi$. Hence the expression for $\frac{{}_oP_{b_o}}{4}$, equation (23e), $= 0$. By inspection the integrand of the first term of this expression is zero, and thus the second integral term is zero. In addition, the second integral term in the expression for $\frac{dy_{cb_o}}{dx}$, equation (23f), is zero since $\frac{{}_oP_b}{4} = 0$.

Finally, consider the special case where $\theta_o = 0$; that is, at the leading edge. Examination of equation (21) reveals that $\frac{{}_oP_b}{4} = 0$ at $\theta_o = 0$. Hence the second integral term in the expression for $\frac{dy_{cb_o}}{dx}$, equation (23f), is zero. Moreover, the second integral term in the expression for $\frac{{}_oP_{bo}}{4}$ is zero by inspection.

Therefore, the expression for $\frac{{}_oP_{bo}}{4}$, equation (23e), and for $\frac{dy_{cbo}}{dx}$, equation (23f), reduce to

$$\frac{{}_oP_{bo}}{4} = \frac{1}{2\pi}\int_0^{\pi}\frac{dy_{cb}}{dx}\left[\operatorname{Cot}\left(\frac{\theta+\theta_o}{2}\right) - \operatorname{Cot}\left(\frac{\theta-\theta_o}{2}\right)\right]d\theta \tag{24a}$$

$$\frac{dy_{cbo}}{dx} = \frac{1}{2\pi}\int_0^{\pi}\frac{{}_oP_b}{4}\left[\operatorname{Cot}\left(\frac{\theta+\theta_o}{2}\right) + \operatorname{Cot}\left(\frac{\theta-\theta_o}{2}\right)\right]d\theta \tag{24b}$$

Let us examine the trignometric portion of the integrand in equation (24a). Rewriting, using known trignometric identities, we have

$$f(\theta)= \frac{\operatorname{Cos}\theta/2\operatorname{Cos}\theta_o/2 - \operatorname{Sin}\theta/2\operatorname{Sin}\theta_o/2}{\operatorname{Sin}\theta/2\operatorname{Cos}\theta_o/2 + \operatorname{Sin}\theta_o/2\operatorname{Cos}\theta/2} - \frac{\operatorname{Cos}\theta/2\operatorname{Cos}\theta_o/2 + \operatorname{Sin}\theta/2\operatorname{Sin}\theta_o/2}{\operatorname{Sin}\theta/2\operatorname{Cos}\theta_o/2 - \operatorname{Sin}\theta_o/2\operatorname{Cos}\theta/2}$$

$$f(\theta)= \frac{\operatorname{Sin}\theta/2\operatorname{Cos}^2\theta_o/2\operatorname{Cos}\theta/2-\operatorname{Sin}^2\theta/2\operatorname{Cos}\theta_o/2\operatorname{Sin}\theta_o/2-\operatorname{Sin}\theta_o/2\operatorname{Cos}\theta_o/2\operatorname{Cos}^2\theta/2}{\operatorname{Sin}^2\theta/2\ \operatorname{Cos}^2\theta_o/2 - \operatorname{Sin}^2\theta_o/2\ \operatorname{Cos}^2\theta/2}$$

$$+\frac{\operatorname{Sin}^2\theta_o/2\operatorname{Sin}\theta/2\operatorname{Cos}\theta/2 - \operatorname{Sin}\theta/2\operatorname{Cos}\theta/2\operatorname{Cos}^2\theta_o/2 - \operatorname{Sin}^2\theta/2\operatorname{Sin}\theta_o/2\operatorname{Cos}\theta_o/2}{\operatorname{Sin}^2\theta/2\ \operatorname{Cos}^2\theta_o/2 - \operatorname{Sin}^2\theta_o/2\ \operatorname{Cos}^2\theta/2}$$

$$+\frac{-\operatorname{Sin}\ \theta_o/2\ \operatorname{Cos}\ \theta_o/2\ \operatorname{Cos}^2\theta/2 - \operatorname{Sin}\ \theta/2\ \operatorname{Cos}\ \theta/2\ \operatorname{Sin}^2\theta_o/2}{\operatorname{Sin}^2\theta/2\ \operatorname{Cos}^2\theta_o/2 - \operatorname{Sin}^2\theta_o/2\ \operatorname{Cos}^2\theta/2}$$

$$= \frac{-2\ \operatorname{Sin}^2\theta/2\ \operatorname{Cos}\ \theta_o/2\ \operatorname{Sin}\ \theta_o/2 - 2\ \operatorname{Sin}\ \theta_o/2\ \operatorname{Cos}\ \theta_o/2\ \operatorname{Cos}^2\theta/2}{\operatorname{Sin}^2\theta/2\ \operatorname{Cos}^2\theta_o/2 - \operatorname{Sin}^2\theta_o/2\ \operatorname{Cos}^2\theta/2}$$

$$f(\theta)= \frac{-\operatorname{Sin}\ \theta_o\ \operatorname{Sin}^2\theta/2 - \operatorname{Sin}\ \theta_o\ \operatorname{Cos}^2\theta/2}{1/4(1-\operatorname{Cos}\ \theta)(1+\operatorname{Cos}\ \theta_o) - 1/4(1-\operatorname{Cos}\ \theta_o)(1+\operatorname{Cos}\ \theta)}$$

$$f(\theta) = \frac{-\operatorname{Sin}\theta_o}{1/4(1+\operatorname{Cos}\theta_o - \operatorname{Cos}\theta - \operatorname{Cos}\theta\operatorname{Cos}\theta_o) - 1/4(1+\operatorname{Cos}\theta - \operatorname{Cos}\theta_o - \operatorname{Cos}\theta_o\operatorname{Cos}\theta)}$$

$$f(\theta) = \frac{-\operatorname{Sin}\theta_o}{1/4(1+\operatorname{Cos}\theta_o - \operatorname{Cos}\theta - \operatorname{Cos}\theta_o\operatorname{Cos}\theta - 1 + \operatorname{Cos}\theta_o - \operatorname{Cos}\theta + \operatorname{Cos}\theta_o\operatorname{Cos}\theta)}$$

$$f(\theta) = \frac{-\operatorname{Sin}\theta_o}{1/4(2\operatorname{Cos}\theta_o - 2\operatorname{Cos}\theta)} = \frac{-\operatorname{Sin}\theta_o}{1/2(\operatorname{Cos}\theta_o - \operatorname{Cos}\theta)}$$

and hence equation (24a) becomes

$$\frac{{}_oP_{b_o}}{4} = \frac{1}{\pi}\int_0^{\pi} \frac{dy_{cb}}{dx} \frac{\operatorname{Sin}\theta_o\, d\theta}{\operatorname{Cos}\theta - \operatorname{Cos}\theta_o} \tag{25a}$$

and in like manner, equation (24b) becomes

$$\frac{dy_{cb_o}}{dx} = -\frac{1}{\pi}\int_0^{\pi} \frac{{}_oP_b}{4} \frac{\operatorname{Sin}\theta\, d\theta}{\operatorname{Cos}\theta - \operatorname{Cos}\theta_o} \tag{25b}$$

which may be useful if the functions under the integrals are expressed as simple functions of θ.

When the functions are expressed in terms of x, the following substitutions reduce equations (25) to a more convenient form:

$x = c/2(1 - \operatorname{Cos}\theta)$	$x_o = c/2(1 - \operatorname{Cos}\theta_o)$
$2x/c = 1 - \operatorname{Cos}\theta$	$2x_o/c = 1 - \operatorname{Cos}\theta_o$
$2x/c - 1 = -\operatorname{Cos}\theta$	$2x_o/c - 1 = -\operatorname{Cos}\theta_o$
$\operatorname{Cos}\theta = 1 - 2x/c$	$\operatorname{Cos}\theta_o = 1 - 2x_o/c$
$d\theta = \dfrac{2\,dx}{c\operatorname{Sin}\theta}$	

And $\quad \cos\theta_o = (1 - 2x_o/c), \quad \sin^2\theta_o = 1 - (\cos\theta_o)^2$

Thus $\quad \sin^2\theta_o = 1 - 1 + 4x_o/c - 4x_o^2/c^2$

So that $\quad \sin\theta_o = 2/c\,\sqrt{x_o(c - x_o)}$

Now substituting into equation (25a) we have

$$\frac{{}_oP_b}{4} = \frac{1}{\pi}\int_0^c \frac{dy_{c_b}}{dx}\,\frac{2/c\,\sqrt{x_o(c - x_o)}\;\,2/c\,dx}{\left[(1 - 2x/c)-(1 - 2x_o/c)\right]\left[2/c\,\sqrt{x(c - x)}\,\right]}$$

$$\frac{{}_oP_b}{4} = -\frac{1}{\pi}\int_0^c \frac{dy_{c_b}}{dx}\,\frac{\sqrt{x_o(c - x_o)}\;dx}{(x - x_o)\;\sqrt{x(c - x)}} \tag{26a}$$

and similarly,

$$\frac{dy_{c_{b_o}}}{dx} = -\frac{1}{\pi}\int_0^c \frac{{}_oP_b}{4}\,\frac{2/c\,\sqrt{x(c - x)}\;\,2/c\,dx}{\left[(1 - 2x/c)-(1 - 2x_o/c)\right]\;\left[2/c\,\sqrt{x(c - x)}\right]}$$

$$\frac{dy_{c_{b_o}}}{dx} = \frac{1}{\pi}\int_0^c \frac{{}_oP_b\;\;dx}{4(x - x_o)} \tag{26b}$$

However, in general the algebraic expressions for ${}_oP_b$ and $\frac{dy_c}{dx}$ are not simple and the direct integrations using equations (25) and (26) are not convenient. Thus it is desirable to perform the integrations numerically using equations (24). The computations may be shortened considerably by use of the following mathematical device:

$$\int_0^{\pi} f(\theta)\,\operatorname{Cot}\left(\frac{\theta + \theta_o}{2}\right)\,d\theta = -\int_{\pi}^{2\pi} f(2\pi - \theta)\,\operatorname{Cot}\left(\frac{\theta - \theta_o}{2}\right)\,d\theta$$

Development of this device is as follows:

Given $I = \int_0^{\pi} f(\theta)\,\mathrm{Cot}\left(\frac{\theta + \theta_0}{2}\right) d\theta$ Let $\theta = 2\pi - x$. When $\theta = 0$, $x = 2\pi$; when $\theta = \pi$, $x = \pi$. Then $f(\theta) = f(2\pi - x)$, and $\mathrm{Cot}\left(\frac{\theta + \theta_0}{2}\right) = \mathrm{Cot}\left(\frac{2\pi - x + \theta_0}{2}\right) = \mathrm{Cot}\left[\pi - \left(\frac{x - \theta_0}{2}\right)\right]$. Now $\mathrm{Cot}\,(\pi - \alpha) = -\mathrm{Cot}\,\alpha$, so that $\mathrm{Cot}\left(\frac{\theta + \theta_0}{2}\right) = -\mathrm{Cot}\left(\frac{x - \theta_0}{2}\right)$. Also $d\theta = -dx$. And therefore we have

$$I = \int_0^{\pi} f(\theta)\,\mathrm{Cot}\left(\frac{\theta + \theta_0}{2}\right) d\theta = \int_{2\pi}^{\pi} f(2\pi - x)\left[-\mathrm{Cot}\left(\frac{x - \theta_0}{2}\right)\right]\left(-dx\right)$$

$$= \int_{2\pi}^{\pi} f(2\pi - x)\,\mathrm{Cot}\left(\frac{x - \theta_0}{2}\right) dx$$

$$= -\int_{\pi}^{2\pi} f(2\pi - x)\,\mathrm{Cot}\left(\frac{x - \theta_0}{2}\right) dx$$

Now the letter representing the variable in any integral makes no difference; hence we replace x by θ. And therefore:

$$\int_0^{\pi} f(\theta)\,\mathrm{Cot}\left(\frac{\theta + \theta_0}{2}\right) d\theta = -\int_{\pi}^{2\pi} f(2\pi - \theta)\,\mathrm{Cot}\left(\frac{\theta - \theta_0}{2}\right) d\theta$$

And now applying the above device to equations (24); where $f(\theta) = \frac{dy_{cb}}{dx}$ and $\frac{{}_oP_b}{4}$ respectively, and $f(2\pi - \theta) = \frac{dy_{cb}}{dx}$ and $\frac{{}_oP_b}{4}$ respectively, we have

$$\frac{{}_oP_{b_0}}{4} = \frac{-1}{2\pi}\int_{\pi}^{2\pi} \frac{+dy_{cb}}{dx}\cdot\mathrm{Cot}\left(\frac{\theta - \theta_0}{2}\right) d\theta \; -\frac{1}{2\pi}\int_0^{\pi} \frac{+dy_{cb}}{dx}\cdot\mathrm{Cot}\left(\frac{\theta - \theta_0}{2}\right) d\theta$$

So that

$$\frac{{}_oP_{b_o}}{4} = -\frac{1}{2\pi}\int_0^{2\pi} \frac{dy_{cb}}{dx} \operatorname{Cot}\left(\frac{\theta - \theta_o}{2}\right) d\theta \tag{27a}$$

$$\text{defining } \left(\frac{dy_{cb}}{dx}\right)_{\pi+\theta} = \left(\frac{dy_{cb}}{dx}\right)_{\pi-\theta}$$

and in the same manner

$$\frac{dy_{cb_o}}{dx} = \frac{1}{2\pi}\int_0^{2\pi} \frac{{}_oP_b}{4} \operatorname{Cot}\left(\frac{\theta - \theta_o}{2}\right) d\theta \tag{27b}$$

$$\text{defining } \left(\frac{{}_oP_b}{4}\right)_{\pi+\theta} = -\left(\frac{{}_oP_b}{4}\right)_{\pi-\theta}$$

These integrals may be evaluated numerically by the method of Reference (4) which is given in Appendix III.

In the preceding theory it was assumed that the airfoil was of infinitesimal thickness, hence the velocity at each elemental vortex along the camber line was taken to be the free-stream velocity V_o. For airfoils of finite thickness, the velocity differs somewhat from V_o. A better approximation is to assume that the velocity at each vortex is the velocity on the surface of the base profile at the same station. Hence, the effect of airfoil thickness will be to change the local lift at x to approximately

$$P = {}_oP\left(\frac{V_f}{V_o}\right)$$

where V_f is the local velocity on the base profile at x. The calculation of V_f is considered elsewhere in this paper.

THE BASE PROFILE THEORY

The problem of determining the velocity distribution over a given base profile or the base profile which will promote a given velocity distribution over its surface may be treated in a manner analogous to that of the mean camber line theory.

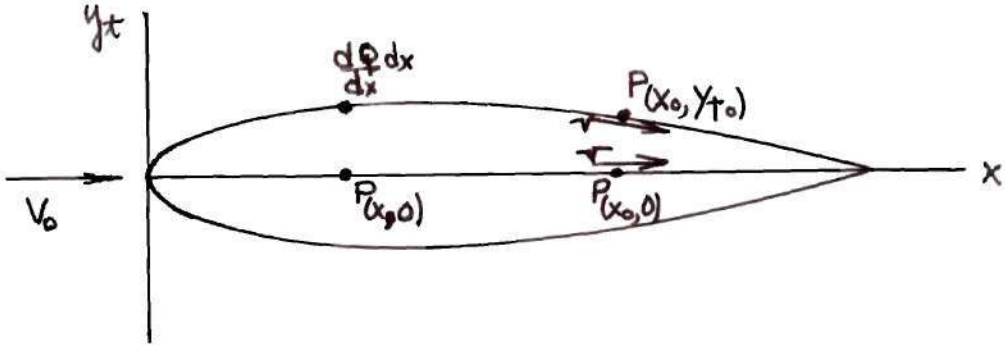

Figure D. Diagram of base profile

Consider the base profile shown in Figure D. If the thickness is small, the velocity induced at a point P (x_0, y_{t_0}) on the surface of the profile by a fluid source or sink at the point P $(x,0)$ is approximately that which would be induced at the point P $(x_0,0)$ by this source or sink. If the source strength at a point x is $(dQ/dx)dx$, then, the velocity induced by all sources or sinks distributed along the x-axis will be

$$v(x_0) = \frac{1}{2\pi}\int_0^c \frac{\frac{dQ}{dx}\,dx}{x_0 - x} \qquad (31)$$

This stems directly from the relation, $v = Q/2\pi r$ in Reference (2).

The source strength can be related to the shape in the following approximate manner: If the profile is thin, the velocity at the surface does not differ materially from the freestream velocity V_o, and hence the flow velocity within the profile due to the sources and sinks is as a first approximation V_o. Within the profile the difference between the quantity of fluid flowing at x + dx and x is the amount supplied by the source contained within this interval, hence

$$\frac{dQ}{dx}\,dx \cong 2V_o\left(y_t + \frac{dy_t}{dx}\,dx\right) - 2V_o y_t.$$

This equation is clarified by Figure E and the following information:

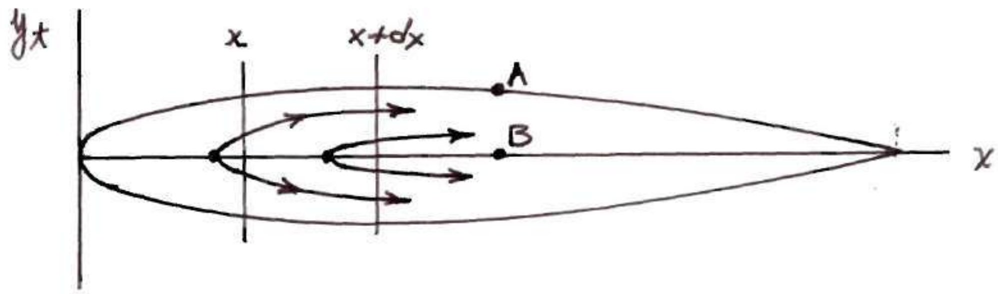

Figure E

The fluid output per source is Q, ft^2/sec in two dimensional analysis. Since the horizontal velocity on the surface and inside the body is essentially V_o, the quantity is $V_o\,y_t$ between points A and B, or $2V_o \cdot y_t$ for the whole airfoil. At x the source strength is $2V_o\,y_t$, and at x + dx the source strength is $2V_o \cdot y_t + 2V_o \frac{dy_t}{dx}\,dx$. Hence the increment in fluid flowing between x + dx and x is given by:

$$\frac{dQ}{dx}\,dx \cong 2V_o\,y_t + 2V_o\frac{dy_t}{dx}\,dx - 2V_o\,y_t$$

or

$$\frac{dQ}{dx}\,dx \cong 2V_o\left(y_t + \frac{dy_t}{dx}\,dx\right) - 2V_o\,y_t$$

and

$$\frac{dQ}{dx} = 2V_o\,\frac{dy_t}{dx} \tag{32}$$

so that equation (31) becomes approximately

$$v/V_o = \frac{1}{\pi}\int_0^c \frac{\frac{dy_t}{dx}\,dx}{x_o - x} \tag{33}$$

By equation (3) we have that

$$x = c/2(1 - \text{Cos } \theta)$$

$$x_o = c/2(1 - \text{Cos } \theta_o)$$

$$dx = c/2 \text{ Sin } \theta \, d\theta$$

and now assuming that the slope of the profile is given by

$$\frac{dy_t}{dx} = B_o' \text{ Cot } \theta/2 + B_o'' \text{ Tan } \theta/2 + \sum_1^{\infty} B_n \text{ Sin } n\theta \tag{34}$$

and thus

$$\frac{dy_t}{dx}\,dx = \left[B_o' \text{ Cot } \theta/2 \text{ Sin } \theta + B_o'' \text{ Tan } \theta/2 \text{ Sin } \theta + \sum_1^{\infty} B_n \text{ Sin } n\theta \text{ Sin } \theta\right] c/2\, d\theta$$

Using the trignometric identities

$$\text{Cot } \theta/2 = \sqrt{\frac{1 + \text{Cos } \theta}{1 - \text{Cos } \theta}}$$

$$\text{Tan } \theta/2 = \sqrt{\frac{1 - \text{Cos } \theta}{1 + \text{Cos } \theta}}$$

$$\text{Sin } \theta = \sqrt{1 - \text{Cos}^2\theta} = \sqrt{(1 + \text{Cos } \theta)(1 - \text{Cos } \theta)}$$

$$\text{Sin } n\theta \text{ Sin } \theta = 1/2 \left[\text{Cos}(n-1)\theta - \text{Cos}(n+1)\theta\right]$$

Then

$$\frac{dyt}{dx}\,dx = c/2\left[B_o'\sqrt{\frac{1+\text{Cos}\,\theta}{1-\text{Cos}\,\theta}}\sqrt{(1+\text{Cos }\theta)(1-\text{Cos }\theta)} + B_o''\sqrt{\frac{1-\text{Cos}\,\theta}{1+\text{Cos}\,\theta}}\sqrt{(1+\text{Cos }\theta)(1-\text{Cos }\theta)}\right.$$

$$\left. + 1/2 \sum_1^\infty B_n \left\{\text{Cos}(n-1)\theta - \text{Cos}(n+1)\theta\right\}\right] d\theta \qquad (34a)$$

Equation (3) yields that: when $x = 0$, $\theta = 0$; when $x = c$, $\theta = \pi$.

And now substituting the above expression for $(dyt/dx)dx$ into equation (33)

$$v/Vo = \frac{1}{\pi}\int_0^\pi \frac{\left[B_o'(1+\text{Cos}\theta) + B_o''(1-\text{Cos}\theta) + 1/2\sum_1^\infty B_n\left\{\text{Cos}(n-1)\theta - \text{Cos}(n+1)\theta\right\}\right]\cdot c/2 \cdot d\theta}{(c/2)(1 - \text{Cos }\theta_o) - (c/2)(1 - \text{Cos }\theta)}$$

$$v/Vo = -\frac{1}{\pi}\int_0^\pi \frac{\left[B_o'(1+\text{Cos}\theta) + B_o''(1-\text{Cos}\theta) + 1/2\sum_1^\infty B_n\left\{\text{Cos}(n-1)\theta - \text{Cos}(n+1)\theta\right\}\right]d\theta}{\text{Cos }\theta_o - \text{Cos }\theta}$$

$$v/Vo = -\frac{1}{\pi}\int_0^\pi \frac{(B_o'+B_o'')\text{Cos}0\theta + (B_o'-B_o'')\text{Cos}\theta\; d\theta}{\text{Cos }\theta_o - \text{Cos }\theta} - \frac{1}{2\pi}\int_0^\pi \frac{\sum_1^\infty B_n\left\{\text{Cos}(n-1)\theta - \text{Cos}(n+1)\theta\right\}d\theta}{\text{Cos }\theta_o - \text{Cos }\theta}$$

However, as previously indicated

$$\int_0^\pi \frac{\text{Cos } n\theta \cdot d\theta}{\text{Cos }\theta_o - \text{Cos }\theta} = -\frac{\pi\,\text{Sin } n\theta_o}{\text{Sin }\theta_o}$$

Now examining the first integral above,

$$I_1 = -\frac{1}{\pi}(B_o' + B_o'')\left(-\pi\frac{\text{Sin } 0\theta_o}{\text{Sin } \theta_o}\right) - \frac{1}{\pi}(B_o' - B_o'')\left(-\pi\frac{\text{Sin } \theta_o}{\text{Sin } \theta_o}\right)$$

$$I_1 = B_o' - B_o''$$

And similarly examining the second integral above,

$$I_2 = -\frac{1}{2\pi}\sum_1^\infty B_n\left[-\frac{\pi\,\text{Sin}(n-1)\theta_o}{\text{Sin } \theta_o} + \frac{\pi\,\text{Sin}(n+1)\theta_o}{\text{Sin } \theta_o}\right]$$

Using the trignometric identity: $\text{Sin A} - \text{Sin B} = 2\text{ Cos}\left[\frac{(A+B)}{2}\right]\cdot$ $\text{Sin}\left[\frac{(A-B)}{2}\right]$ we have $\text{Sin }(n+1)\theta_o - \text{Sin }(n-1)\theta_o =$

$2\text{ Cos}\left[\frac{(n+1+n-1)\theta_o}{2}\right]\text{ Sin}\left[\frac{(n+1-n+1)\theta_o}{2}\right] = 2\text{ Cos } n\theta_o\text{ Sin }\theta_o.$

And thus $I_2 = \frac{-1}{2\pi}\sum_1^\infty B_n\pi\frac{2\text{ Cos } n\theta_o\text{ Sin }\theta_o}{\text{Sin }\theta_o} = -\sum_1^\infty B_n\text{ Cos } n\theta_o.$ Now combining I_1 and I_2 we have for the velocity ratio at any general value of θ

$$v/Vo = B_o' - B_o'' - \sum_1^\infty B_n\text{ Cos } n\theta \qquad (35)$$

And now integrating equation (35) from 0 to π,

$$\int_0^\pi v/Vo\, d\theta = \int_0^\pi (B_o' - B_o'')\, d\theta - \int_0^\pi \sum_1^\infty B_n\text{ Cos } n\theta\, d\theta$$

Therefore

$$\int_0^\pi \frac{v}{Vo}\, d\theta = (B_o' - B_o'')\pi - \sum_1^\infty B_n\frac{\text{Sin } n\theta}{n}\Bigg]_0^\pi$$ The last term here

vanishes for all values of n so that

$$B_o' - B_o'' = \frac{1}{\pi}\int_0^\pi \frac{v}{Vo}\, d\theta \qquad (36a)$$

To find the general Fourier coefficient B_n, multiply equation (35) by $\cos n\theta$ and integrate from 0 to π. Thus

$$\int_0^{\pi} \frac{v}{V_o} \cos n\theta \, d\theta = \int_0^{\pi} (B_o' - B_o'')\cos n\theta \, d\theta - B_n \int_0^{\pi} \cos^2 n\theta \, d\theta \quad \text{since}$$

all the Cosine products vanish upon integration from θ to π except $\cos n\theta \cos n\theta$.

$$\int_0^{\pi} \frac{v}{V_o} \cos n\theta \, d\theta = \frac{1}{n} (B_o - B_o) \sin n\theta \Big]_0^{\pi} - \frac{B_n}{2} \left(\theta + \frac{\sin 2n\theta}{2n}\right)\Big]_0^{\pi}$$

$$\int_0^{\pi} \frac{v}{V_o} \cos n\theta \, d\theta = \frac{-B_n}{2} (\pi)$$

Therefore

$$B_n = \frac{-2}{\pi} \int_0^{\pi} \frac{v}{V_o} \cos n\theta \, d\theta \tag{36b}$$

The condition that the trailing edge shall close is that the summation of the vertical ordinate increments from the leading edge to the trailing edge shall be zero. That is

$$\int_0^{\pi} dy_t = \int_0^{\pi} \frac{dy_t}{dx} \, dx = 0$$

Substituting the slope as given by equation (34a) into the above expression and integrating from 0 to π, it follows that

$$\int_0^{\pi} \left[B_o'(1+\cos\theta) + B_o''(1-\cos\theta) + 1/2 \sum_1^{\infty} B_n \left\{ \cos(n-1)\theta - \cos(n+1)\theta \right\} \right] c/2 \, d\theta = 0.$$

$$\int_0^{\pi}\left[(B_o'+B_o'')\ \mathrm{Cos}\ 0\theta + (B_o'-B_o'')\ \mathrm{Cos}\ \theta + 1/2\sum_1^{\infty} B_n\left\{\mathrm{Cos}(n-1)\theta - \mathrm{Cos}(n+1)\theta\right\}\right]c/2\ d\theta = 0$$

And performing the integration, we have

$$\theta\frac{c}{2}(B_o'+B_o'')\Big]_0^{\pi} + \frac{c}{2}(B_o'-B_o'')\ \mathrm{Sin}\ \theta\Big]_0^{\pi} + 1/2\sum_1^{\infty} B_n\left(\frac{\mathrm{Sin}(n-1)\theta}{n-1} - \frac{\mathrm{Sin}(n+1)\theta}{n+1}\right)\Big]_0^{\pi}\frac{c}{2} = 0.$$

Now as shown in the development of equation (10), the $\sum_1^{\infty} B_n$ term above vanishes for all n except $n = 1$. For this value of n, it has been demonstrated that the value of the expression $= \frac{c}{2} B_1 \pi$.

Therefore $\quad \frac{c}{2}(B_o' + B_o'')\pi + 1/2\ B_1(\pi)\frac{c}{2} = 0.$

And thus $\quad B_o' + B_o'' + 1/2\ B_1 = 0.$ (37)

An examination of equations (34) and (35) reveals that these equations may be used to find the shape of the base profile corresponding to a given velocity distribution or inversely, the velocity distribution corresponding to a given base profile shape. However, equation (34) for the base profile shape becomes infinite for $\theta = 0$ and $\theta = \pi$; that is, at the leading edge and at the trailing edge. We avoid this undesirable phenomena by utilizing the method of superposition and select a known profile as a base and thus compute the values of $\frac{d\Delta y_t}{dx}$ and $\frac{\Delta v}{V_o}$ with respect to this base profile. Addition of the values of $\frac{d\Delta y_t}{dx}$ and $\frac{\Delta v}{V_o}$ calculated from equations (34) and (35) with respect to the base profile to the known values of $\frac{dy_t}{dx}$ and $\frac{v}{V_o}$ for this reference base profile yields the desired values. Now the immense value of this method of obtaining the desired base profile shape and velocity distribution is the fact that by proper selection of the reference base profile so that it possesses the same slope characteristics as the actual profile under consideration at the leading edge and trailing edge, and letting Δy_t represent the change in shape from the reference profile to the profile under consideration, we have from equation (34) at the leading and trailing edges respectively:

$$\frac{d\Delta y_t}{dx} = 0 = B_o' \operatorname{Cot} \frac{0}{2} + B_o'' \operatorname{Tan} \frac{0}{2} + \sum_1^\infty B_n \operatorname{Sin} n0$$

$$\frac{d\Delta y_t}{dx} = 0 = B_o' \operatorname{Cot} \frac{\pi}{2} + B_o'' \operatorname{Tan} \frac{\pi}{2} + \sum_1^\infty B_n \operatorname{Sin} n\pi$$

Thus the coefficients B_o' and B_o'' must be identically zero to satisfy the above equations. Now letting Δv represent the change in velocity from the reference profile to the profile under consideration, we may rewrite equations (34) and (35) as follows:

$$\frac{d\Delta y_t}{dx} = \sum_1^\infty B_n \operatorname{Sin} n\theta$$

$$\frac{\Delta v}{V_o} = -\sum_1^\infty B_n \operatorname{Cos} n\theta \qquad (40)$$

and the coefficients, which may be developed in the identical manner as shown in equations (22a) and (22b), are

$$B_n = \frac{2}{\pi} \int_0^\pi \frac{d\Delta y_t}{dx} \operatorname{Sin} n\theta \, d\theta$$

or (41)

$$B_n = \frac{-2}{\pi} \int_0^\pi \frac{\Delta v}{V_o} \operatorname{Cos} n\theta \, d\theta$$

It is apparent from equation (37) that the coefficient B_1 must be zero since B_0' and B_0'' are both zero. Therefore when it is desired to find a change in base profile shape corresponding to a given change in the velocity distribution, having established the condition that $B_0' = B_0'' = B_1 = 0$, it is evident from equations (36) that the change in velocity distribution must be so chosen that the conditions

$$\int_0^{\pi} \frac{\Delta v}{V_o} \, d\theta = 0 \tag{42}$$

and

$$\int_0^{\pi} \frac{\Delta v}{V_o} \cos \theta \, d\theta = 0$$

must be satisfied if the velocity distribution chosen is to correspond to a real base profile.

Using equation (40) and (41) the chordwise velocity distribution corresponding to a given base profile or the base profile corresponding to a given velocity distribution may be found. The calculations will in general be very lengthy so that it is desirable to replace the expansions by integral expressions as was done in the development of the method of the mean camber line theory. Thus substitution of the expressions for the Fourier coefficients given by equations (41) into the equations (40) yields that at θ_o:

$$\frac{d \Delta y_{t_o}}{dx} = \frac{-2}{\pi} \int_0^{\pi} \frac{\Delta v}{V_o} \sum_1^{\infty} \cos n\theta \sin n\theta_o \, d\theta \tag{42a}$$

$$\frac{\Delta v_o}{V_o} = \frac{-2}{\pi}\int_0^{\pi}\frac{d\,\Delta y_t}{dx}\sum_1^{\infty}\text{Sin } n\theta \text{ Cos } n\theta_o \, d\theta$$

Now

$$\text{Sin } n\theta_o \text{ Cos } n\theta = \frac{1}{2}\left[\text{Sin } n(\theta+\theta_o) - \text{Sin } n(\theta-\theta_o)\right]$$
$$\text{Sin } n\theta \text{ Cos } n\theta_o = \frac{1}{2}\left[\text{Sin } n(\theta+\theta_o) + \text{Sin } n(\theta-\theta_o)\right] \tag{42b}$$

and further, it is given in References (4) and (5) that

$$\sum_1^{n}\text{Sin } n\,(\theta \pm \theta_o) = \frac{1}{2}\text{Cot}\left(\frac{\theta \pm \theta_o}{2}\right) - \frac{\text{Cos }(2n+1)\left(\frac{\theta \pm \theta_o}{2}\right)}{2\text{ Sin }\left(\frac{\theta \pm \theta_o}{2}\right)} \tag{42c}$$

so that substitution of equations (42b) into equations (42a) gives

$$\frac{d\,\Delta y_{t_o}}{dx} = \frac{-2}{\pi}\int_0^{\pi}\frac{\Delta v}{V_o}\sum_1^{\infty}\frac{1}{2}\left[\text{Sin } n(\theta+\theta_o) - \text{Sin } n(\theta-\theta_o)\right] d\theta$$

$$\frac{\Delta v_o}{V_o} = \frac{-2}{\pi}\int_0^{\pi}\frac{d\,\Delta y_t}{dx}\sum_1^{\infty}\frac{1}{2}\left[\text{Sin } n(\theta+\theta_o) + \text{Sin } n(\theta-\theta_o)\right] d\theta$$

and now substituting equation (42c) into the above expressions

$$\frac{d\Delta y_{t_o}}{dx} = \lim_{n\to\infty}\left\{\frac{-1}{2\pi}\int_0^{\pi}\frac{\Delta v}{V_o}\left[\text{Cot}\left(\frac{\theta+\theta_o}{2}\right) - \text{Cot}\left(\frac{\theta-\theta_o}{2}\right)\right] d\theta\right.$$
$$\left. + \frac{1}{2\pi}\int_0^{\pi}\frac{\Delta v}{V_o}\left[\frac{\text{Cos}(2n+1)\left(\frac{\theta+\theta_o}{2}\right)}{\text{Sin}\left(\frac{\theta+\theta_o}{2}\right)} - \frac{\text{Cos}(2n+1)\left(\frac{\theta-\theta_o}{2}\right)}{\text{Sin}\left(\frac{\theta-\theta_o}{2}\right)}\right] d\theta\right\} \tag{42d}$$

and similarly:

$$\frac{\Delta v_o}{Vo} = \lim_{n\to\infty}\left\{\frac{-1}{2\pi}\int_0^{\pi}\frac{d\,\Delta yt}{dx}\left[\operatorname{Cot}\left(\frac{\theta+\theta_o}{2}\right) + \operatorname{Cot}\left(\frac{\theta-\theta_o}{2}\right)\right]d\theta\right.$$

$$\left. + \frac{1}{2\pi}\int_0^{\pi}\frac{d\Delta yt}{dx}\left[\frac{\operatorname{Cos}(2n+1)\left(\frac{\theta+\theta_o}{2}\right)}{\operatorname{Sin}\left(\frac{\theta+\theta_o}{2}\right)} + \frac{\operatorname{Cos}(2n+1)\left(\frac{\theta-\theta_o}{2}\right)}{\operatorname{Sin}\left(\frac{\theta-\theta_o}{2}\right)}\right]d\theta\right\} \qquad (42e)$$

In the limit the second integrals in the above relations become zero, as shown previously in the development of equations (24a) and (24b), and thus the equations may be written as:

$$\frac{d\,\Delta yt_o}{dx} = \frac{-1}{2\pi}\int_0^{\pi}\frac{\Delta v}{Vo}\left[\operatorname{Cot}\left(\frac{\theta+\theta_o}{2}\right) - \operatorname{Cot}\left(\frac{\theta-\theta_o}{2}\right)\right]d\theta$$

$$\frac{\Delta v_o}{Vo} = \frac{-1}{2\pi}\int_0^{\pi}\frac{d\,\Delta yt}{dx}\left[\operatorname{Cot}\left(\frac{\theta+\theta_o}{2}\right) + \operatorname{Cot}\left(\frac{\theta-\theta_o}{2}\right)\right]d\theta \qquad (42f)$$

For the occasions when the change in shape or velocity distribution is known as a relatively simple trigonometric function in θ, it is sometimes convenient to use the equations

$$\frac{d\,\Delta yt_o}{dx} = \frac{-1}{\pi}\int_0^{\pi}\frac{\Delta v}{Vo}\,\frac{\operatorname{Sin}\theta_o\,d\theta}{\operatorname{Cos}\theta - \operatorname{Cos}\theta_o} \qquad (43)$$

and

$$\frac{\Delta v_o}{Vo} = \frac{1}{\pi}\int_0^{\pi}\frac{d\,\Delta yt}{dx}\,\frac{\operatorname{Sin}\theta\,d\theta}{\operatorname{Cos}\theta - \operatorname{Cos}\theta_o}$$

which are derived from equations (42f) in the identical manner as in the development of equations (25a) and (25b).

When the change in shape or velocity distribution is known as a relatively simple function of x, then it may be convenient to use the equations

$$\frac{d\Delta y t_o}{dx} = \frac{1}{\pi}\int_0^c \frac{\Delta v/Vo \ \sqrt{x_o(c - x_o)} \ dx}{(x - x_o)\sqrt{x(c - x)}} \qquad (44)$$

$$\frac{\Delta v}{Vo} = \frac{-1}{\pi}\int_0^c \frac{\frac{d\Delta yt}{dx} \ dx}{x - x_o}$$

which are developed from equations (43) in the same way that equations (26) are derived from equations (25) as previously shown.

Again utilizing the mathematical device

$$\int_0^{\pi} f(\theta)\ \mathrm{Cot}\left(\frac{\theta + \theta_o}{2}\right)d\theta = -\int_{\pi}^{2\pi} f(2\pi - \theta)\ \mathrm{Cot}\left(\frac{\theta - \theta_o}{2}\right) d\theta$$

where $f(\theta) = \frac{\Delta v}{Vo}$ and $\frac{d\Delta yt}{dx}$ respectively; and $f(2\pi - \theta) = \frac{\Delta v}{Vo}$ and $\frac{d\Delta yt}{dx}$ respectively, we have from equations (42f)

$$\frac{d\Delta yt_o}{dx} = \frac{-1}{2\pi}\left[-\int_{\pi}^{2\pi}\frac{\Delta v}{Vo}\ \mathrm{Cot}\left(\frac{\theta - \theta_o}{2}\right)d\theta - \int_0^{\pi}\frac{\Delta v}{Vo}\ \mathrm{Cot}\left(\frac{\theta - \theta_o}{2}\right)d\theta\right]$$

$$\frac{\Delta v_o}{Vo} = \frac{-1}{2\pi}\left[-\int_{\pi}^{2\pi}\frac{d\Delta yt}{dx}\ \mathrm{Cot}\left(\frac{\theta - \theta_o}{2}\right)d\theta + \int_0^{\pi}\frac{d\Delta yt}{dx}\ \mathrm{Cot}\left(\frac{\theta - \theta_o}{2}\right)d\theta\right]$$

which may be written as follows:

$$\frac{d\,\Delta y_{t_o}}{dx} = \frac{1}{2\pi}\int_0^{2\pi} \frac{\Delta v}{V_o}\,\mathrm{Cot}\left(\frac{\theta - \theta_o}{2}\right) d\theta$$

$$\text{defining } \left(\frac{\Delta v}{V_o}\right)_{\pi+\theta} = \left(\frac{\Delta v}{V_o}\right)_{\pi-\theta} \tag{45}$$

and

$$\frac{\Delta v_o}{V_o} = \frac{-1}{2\pi}\int_0^{2\pi} \frac{d\,\Delta y_t}{dx}\,\mathrm{Cot}\left(\frac{\theta - \theta_o}{2}\right) d\theta$$

$$\text{defining } \left(\frac{d\,\Delta y_t}{dx}\right)_{\pi+\theta} = -\left(\frac{d\,\Delta y_t}{dx}\right)_{\pi-\theta}$$

These integrals may be evaluated numerically by the method of Reference (4) which is given in Appendix III.

APPLICATION OF THE THEORY TO THE PROBLEM OF DETERMINING THE AIRFOIL CORRESPONDING TO A GIVEN VELOCITY DISTRIBUTION

General Procedure

The desired velocity distribution is selected and the corresponding velocity distribution over the base profile is found by averaging the upper and lower surface velocities at each chordwise station. It is to be noted that the shape of a two-dimensional body corresponding to the desired velocity distribution may not represent a real airfoil section which is both "closed" and "pointed" at the trailing edge. Thus the base profile corresponding to the desired velocity distribution will, in general, be modified slightly to conform to a real profile. After this adjustment, the base profile shape corresponding to the corrected base profile velocity distribution is calculated. It is important to note that any slight change to the original base profile in making the adjustment to a real profile necessitates corresponding changes in the original velocity distribution, and thus the desired velocity distribution will, in general, be modified slightly to conform to the adjusted base profile. Usually, these changes are small and will not affect the utility of either the velocity distribution or the airfoil. The chordwise pressure distribution is calculated from the adjusted upper and lower surface velocity distributions. Then the chordwise pressure distribution for the airfoil with the thickness removed is determined and the mean camber line shape is calculated. Finally, the calculated mean camber line and base profile shapes are combined to give the airfoil section shape corresponding to the modified velocity distribution. All the steps outlined above are presented in detail in the following pages.

Detailed Procedure

In general, it is required that the airfoil corresponding to the desired velocity distribution be one having a specified thickness ratio. This requirement - together with the requirement that the desired velocity distribution correspond to that for a real airfoil section which is both closed and pointed at the trailing edge - complicates the problem since it is not apparent from the velocity distribution whether the requirements are fulfilled. By choosing the velocity distribution wisely these difficulties can largely be eliminated. Of particular value is reference to known velocity distributions over existing airfoils having similar thickness ratios and velocity distributions to those desired.

Figure 1 defines the desired velocity distributions for upper and lower surfaces. (This is the theoretical velocity distribution for the NACA 66(215)-216 airfoil given in Reference (6). This same reference includes the ordinates for the airfoil.) Having thus defined the desired velocity distribution, it is further specified that the airfoil to be derived shall be of approximately 16 per cent thickness. Therefore, the calculated airfoil may be compared with the actual airfoil corresponding to the desired velocity distribution.

It is necessary that existing airfoil data be examined and from these data to select an airfoil whose upper surface velocity distribution is very similar to the desired upper surface velocity distribution; and similarly, selection of a second airfoil whose lower surface velocity distribution is very similar to the desired lower surface velocity distribution. Figure 2 illustrates this procedure. The similar airfoils selected are the NACA 66_4-021 upper surface velocity distribution for $C_l = 0$ and the NACA 66,1-012 lower surface velocity distribution for $C_l = 0$. These airfoils and data are available in Reference (6). The reason for introducing these similar airfoils is to facilitate selection of a reference base profile from a table of Joukowski base profiles in Reference (1). Now the airfoil to be derived will obviously have a leading edge radius approximately midway between that for an NACA 66_4-021 and the NACA 66,1-012 airfoils. The leading edge radii for these two respectively are:

$$r/c = .02550$$

$$r/c = .00893$$

and thus the average radius is $r/c = .01722$. Now using this average leading edge radius as a guide, we select a Joukowski base profile from Table II of Reference (1) that has a leading edge radius of approximately the same magnitude. The Joukowski base profile for which $t/c = 0.12$ has nearly this radius (.01706) and is therefore used as the reference base profile.

By computing the average of the desired upper and lower surface velocity distributions $(V_u/V_o)_1$ and $(V_l/V_o)_1$ respectively, at various chordwise stations the base profile velocity distribution $(V_f/V_o)_1$ is obtained. The subscript (1) is used to denote that these velocity distributions are a first trial and are subject to slight modifications. Figure 2 shows the base profile velocity distribution, $(V_f/V_o)_1$.

The difference between the desired and the reference base profiles is found from

$$\left(\frac{\Delta v}{V_o}\right)_1 = \left(\frac{V_f}{V_o}\right)_1 - \left(\frac{V_r}{V_o}\right)$$

The values of $\left(\frac{\Delta v}{V_o}\right)_1$ are found in Table I for the usual values of x/c. Values of θ and Cos θ corresponding to various values of x/c are conveniently available in Table V, Reference (1). Values of $\left(\frac{\Delta v}{V_o}\right)_1 \times \cos\theta$ are calculated as shown in Table I. Then both $\left(\frac{\Delta v}{V_o}\right)_1$ and $\left(\frac{\Delta v}{V_o}\right)_1 \times \cos\theta$ are plotted as functions of θ in Figure 3.

It is now necessary to make some adjustments to the first choice velocity distributions. That is, we employ the fact that - in order for the desired velocity distribution to represent a real airfoil which closes and has a sharp trailing edge - it is required that the relations

$$\int_0^{\pi} \frac{\Delta v}{V_o}\, d\theta = 0$$

$$\int_0^{\pi} \frac{\Delta v}{V_o} \cos\theta \, d\theta = 0$$

be satisfied. These conditions are discussed elsewhere in this writing, (loc. cit. equations (42)), and are not satisfied since a theoretical velocity distribution, not the true velocity distribution, for the NACA 66(215)-216 airfoil was utilized as the desired distribution of velocity.

Using a planimeter the area under the $\left(\frac{\Delta v}{V_o}\right)_1$ curve is integrated from 0 to π and it is found that

$$\int_0^{\pi} \left(\frac{\Delta v}{V_o}\right)_1 d\,\theta = -.0268$$

Similarly, the area under the $\left(\frac{\Delta v}{V_o}\right)_1 \times \text{Cos}\,\theta$ curve is integrated from 0 to π with the result that

$$\int_0^{\pi} \left(\frac{\Delta v}{V_o}\right)_1 \times \text{Cos}\,\theta\, d\,\theta = -.0277$$

Obviously, an adjustment of the curves is necessary. The second trial, designated $\left(\frac{\Delta v}{V_o}\right)_2$ and thus $\left(\frac{\Delta v}{V_o}\right)_2 \times \text{Cos}\,\theta$, is an estimate based on inspection of the above results and the characteristics of the curves in Figure 3. Again the mechanical integrations are performed and we have

$$\int_0^{\pi} \frac{\Delta v}{V_o}\, d\,\theta = .005200$$

$$\int_0^{\pi} \frac{\Delta v}{V_o} \times \text{Cos}\,\theta\, d\,\theta = .001532$$

Hence, the conditions are nearly satisfied. In order to completely satisfy the conditions, it is strongly recommended that the method of final correction defined in Reference (1) be utilized. This eliminates the undesirable trial and error procedure otherwise necessary at this point. Therefore, according to Reference (1), the conditions may be satisfied completely by slightly translating and rotating the second trial of $\frac{\Delta v}{V_o}$. Assuming that a small increment

$$\Delta\left(\frac{\Delta v}{V_o}\right) = k_1 + k_2\left(\frac{\pi}{2} - \theta\right) \qquad (64)$$

be added to the distribution $\left(\frac{\Delta v}{V_o}\right)_2$ since

$$\left.\begin{aligned} &\int_0^{\pi} \Delta\left(\frac{\Delta v}{V_o}\right) d\,\theta = \pi k_1 \\ \text{and} \qquad &\int_0^{\pi} \Delta\left(\frac{\Delta v}{V_o}\right) \operatorname{Cos}\theta \, d\,\theta = 2\,k_2 \end{aligned}\right\} \tag{65}$$

then making

$$k_1 = \frac{-.005200}{\pi} = -.00166$$

and

$$k_2 = \frac{-.001532}{2} = -.000766$$

the velocity distribution

$$\frac{\Delta v}{V_o} = \left(\frac{\Delta v}{V_o}\right)_2 + \Delta\left(\frac{\Delta v}{V_o}\right) \tag{66}$$

will completely satisfy the requirements. In Table I the values of

$$\Delta\left(\frac{\Delta v}{V_o}\right) = -.00166 - .00766\left(\frac{\pi}{2} - \theta\right)$$

are given and the final value of the difference velocity distribution $\frac{\Delta v}{V_o}$ is calculated using equation (66).

It is now possible to calculate the base profile ordinates. The procedure here is to calculate values of $\frac{d\,\Delta y_t}{d\,x}$ by numerical integration of equation (45); then by plotting $\frac{d\,\Delta y_t}{d\,x}$ versus x/c and mechanically integrating find the values $\frac{\Delta y_t}{c}$, which finally yield values of the base profile ordinates y_t from

$$\frac{y_t}{c} = \frac{y_r}{c} + \frac{\Delta y_t}{c} \tag{67}$$

which corresponds to the base profile velocity distribution

$$\frac{V_f}{V_o} = \frac{V_r}{V_o} + \frac{\Delta v}{V_o}\,. \tag{68}$$

The method of numerical integration of equation 45 is illustrated in Reference (1). For convenience, the method is given in Appendix III of this writing. Tables II and III present the complete calculation of $\frac{d\Delta y_t}{d\,x}$ and are carefully explained in Appendix I.

Now having obtained values of $\frac{d\Delta y_t}{d\,x}$, these values are plotted as a function of x/c as shown in Figure 4. By mechanical integration with a planimeter the curve in Figure 4 is integrated to each desired value of x/c and thus the value of $\frac{\Delta y_t}{c}$ is obtained at the desired chordwise stations. Having values of $\frac{\Delta y_t}{c}$ and corresponding values of $\frac{y_r}{c}$, the base profile ordinates are obtained from

$$\frac{y_t}{c} = \frac{y_r}{c} + \frac{\Delta y_t}{c} \tag{67}$$

and these ordinates correspond to the base profile velocity distribution, $\frac{V_f}{V_o}$ which is found from

$$\frac{V_f}{V_o} = \frac{V_r}{V_o} + \frac{\Delta v}{V_o} \tag{68}$$

Values of $\frac{V_f}{V_o}$ are given in Table I. The base profile ordinates are plotted in Figure 5.

In this particular calculation the maximum thickness is approximately 16 per cent of the chord as was desired. In the event that the calculated thickness t_1 is different from the required thickness t_2, then the ordinates and velocity distribution for the base profile of thickness t_2 can be obtained from the following:

$$\left(\frac{y_t}{c}\right)_2 = \frac{t_2}{t_1}\left(\frac{y_t}{c}\right)_1 \tag{69}$$

$$\left(\frac{V_f}{V_o}\right)_2 = 1 + \frac{t_2}{t_1}\left[\left(\frac{V_f}{V_o}\right) - 1\right] \tag{70}$$

Now at this stage in the calculation of the airfoil corresponding to the desired velocity distribution it is necessary to revise the desired velocity distribution so as to account for the changes made to the original base profile velocity distribution $\left(\frac{V_f}{V_o}\right)_1$ to make that distribution represent a real profile. This, it is believed, is best accomplished graphically on the plot of the corrected base profile velocity distribution. The writer used a different method based on the following equations:

$$\left.\begin{aligned} \frac{V_u}{V_o} &= \frac{V_f}{V_o} + \frac{P_b/4}{V_f/V_o} \\ \frac{V_l}{V_o} &= \frac{V_f}{V_o} - \frac{P_b/4}{V_f/V_o} \end{aligned}\right\} \tag{71}$$

Correction of the original upper and lower surface velocity distributions was accomplished by specifying that the original upper surface velocity distribution $(V_u/V_o)_1$ was not to be changed and thus all the correction was absorbed into the lower surface velocity distribution. Thus the basic pressure distribution $P_b/4$ was computed from

$$\frac{V_u}{V_o} = \frac{V_f}{V_o} + \frac{P_b/4}{V_f/V_o} \qquad (71)$$

since it is the only unknown involved. Hence the corrected lower surface velocity distribution was calculated from

$$\frac{V_l}{V_o} = \frac{V_f}{V_o} - \frac{P_b/4}{V_f/V_o} \qquad (71)$$

Table IV presents results of these calculations.

In general this method of correcting the original velocity distributions is satisfactory if a plot of the corrected distributions is made and compared with the desired distributions and it is determined that the changes in the V_l/V_o distribution are not unsatisfactory. The importance of this procedure was not evident to the writer since it was assumed that the changes to the desired velocity distribution would be small. Usually this is true, but by the above method the lower surface distribution alone absorbs all the change, and it was later found that, in this case, the resulting corrected V_l/V_o distribution was not particularly desirable. This is apparent in Figure 6 where it is evident that the lower surface distribution is no longer laminar to the 60% chord station as was desired. The laminar flow is lost at about the 20% chord station.

It is to be noted, however, that the preceding method is very useful if it were important to maintain either the upper or lower surface original velocity distributions, and as stated previously, it is also satisfactory if the resulting corrections to one surface are not undesirable.

However, the graphical method by direct examination of the corrected base profile velocity distribution curve in conjunction with the desired distribution curves is satisfactory at all times and has the advantage that it is apparent whether or not the changes to the desired curves are satisfactory.

Figure 6, therefore, is the new desired velocity distribution for which the airfoil will be derived.

We now proceed to the calculation of the mean camber line ordinates. In this calculation the basic pressure distribution corresponding to zero profile thickness ${}_oP_b$ must be used. We have from equation (54) of Reference (1) that

$$ {}_oP_b = \frac{P_b}{V_f/V_o} \tag{54} $$

and hence by virtue of equation (71) this distribution can be obtained directly from

$$ {}_oP_b = 2\left(\frac{V_u}{V_o} - \frac{V_l}{V_o}\right) \tag{73} $$

Values of ${}_oP_b$ and P_b are shown in Table V.

The problem is therefore to determine the mean camber line shape which will promote the above basic pressure distribution. The procedure here is to calculate values of $\frac{d\,y_{c_b}}{d\,x}$ by numerical integration of equation (27); then by plotting $\frac{d\,y_{c_b}}{d\,x}$ versus x/c and mechanically integrating find the values $\frac{y_{c_b}}{c}$. The final step is to correct these values of $\frac{y_{c_b}}{c}$

which are with reference to the ideal angle of attack, α_i, to the regular coordinate system consisting of the x-y axes.

The method of numerical integration of equation (27) has previously been discussed. Figure 7 is the required plot of $\frac{P_b}{q}/4$ versus θ, and Tables VI and VII present the complete calculation of $\frac{d\,y_{c_b}}{d\,x}$ and are explained in detail in Appendix I.

Upon obtaining the values of $\frac{d\,y_{c_b}}{d\,x}$, these values are plotted as a function of x/c as shown in Figure 8. By mechanical integration employing a planimeter the curve in Figure 8 is integrated to each desired value of x/c and thus the value of y_{c_b} is obtained at the desired chordwise stations. Table V presents the values of y_{c_b}.

The mean camber line thus obtained is at the ideal angle of attack; that is, the ordinates obtained are referenced to the angle of attack for which the additional pressure distribution is zero; and hence, unless the ideal angle is zero, the trailing edge is either below or above the x/c axis. Ordinates of camber lines are generally specified with the extremities of the camber line on the x/c axis and designated by the usual symbol y_c.

Now the ideal angle of attack is simply

$$\alpha_i = \left(\frac{y_{c_b}}{c}\right)_{\frac{x}{c}=0} - \left(\frac{y_{c_b}}{c}\right)_{\frac{x}{c}=1.0} \tag{74}$$

and

$$\frac{y_c}{c} = \frac{y_{c_b}}{c} + \frac{x}{c}\,\alpha_i \tag{75}$$

$$\frac{dy_c}{dx} = \frac{dy_{cb}}{dx} + \alpha_i \tag{75}$$

The above relations may be verified from an inspection of Figure C given elsewhere in this paper. The value of α_i in this calculation is .00424 radians = $.25^\circ$. Values of the mean camber line ordinates are given in Table V, and Figure 9 is a plot of the mean camber line.

Therefore, having both the values of the base profile ordinates, $\frac{y_t}{c}$, and the mean camber line ordinates, $\frac{y_c}{c}$, it is now possible to calculate the airfoil ordinates from the following relations:

$$\begin{aligned}
\frac{x_u}{c} &= \frac{x}{c} - \frac{y_t}{c}\,\mathrm{Sin}\,\beta \\
\frac{y_u}{c} &= \frac{y_c}{c} + \frac{y_t}{c}\,\mathrm{Cos}\,\beta \\
\frac{x_l}{c} &= \frac{x}{c} + \frac{y_t}{c}\,\mathrm{Sin}\,\beta \\
\frac{y_l}{c} &= \frac{y_c}{c} - \frac{y_t}{c}\,\mathrm{Cos}\,\beta
\end{aligned} \tag{76}$$

where

$$\beta = \mathrm{Tan}^{-1}\left(\frac{dy_c}{dx}\right).$$

The above relations may be verified from an inspection of the following diagram, Figure F, where the camber line is greatly exaggerated for clarity.

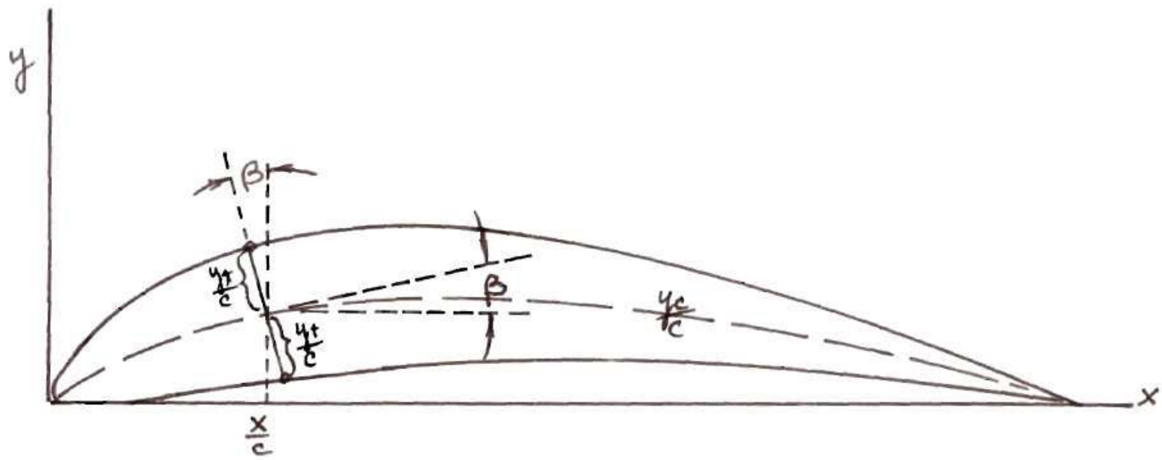

Figure F.

Calculation of the final airfoil coordinates is presented in Table VIII, and the resulting airfoil is plotted in Figure 10. Also shown in Figure 10 is the plot of the NACA 66(215)-216 airfoil corresponding to the original desired velocity distribution.

EXPERIMENTAL APPARATUS, TESTS, AND RESULTS

In order to test the validity of the theory, a suitable model of the derived airfoil was constructed for the purpose of obtaining the actual velocity distribution over the airfoil, and hence to compare the actual distribution with the desired distribution.

Apparatus

The model constructed was of laminated mahogany, with a 10 inch chord and a 30 inch span. Pressure orifices were situated at the desired chordwise locations on upper and lower surfaces. The tests were conducted in the small, low-speed wind tunnel at the Georgia Institute of Technology. Figure 12 illustrates both the configuration of the model and the installation of the model in the wind tunnel. Figure 13 is a study of the tunnel test section, and of the auxiliary apparatus. Pressures over the wing were observed on the alcohol manometer bank shown in Figure 13. The tunnel control panel and the alcohol manometer indicating velocity in the jet are also shown in Figure 13.

Tests

All of the tests were two dimensional and were conducted with the test section closed as shown in Figures 12 and 13. The indicated velocity was 80.5 mph corresponding to a true velocity of 83.6 mph and to a tunnel Reynolds Number of 579,000. These calculations are presented in detail in Appendix IV. This Reynolds Number must be corrected for the effects of tunnel turbulence by the relation

$$R\,N_e = T\,F \times R\,N$$

where $R\,N_e$ is the effective Reynolds Number of the airfoil, and $T\,F$ is the tunnel turbulence factor, Reference (7). For this tunnel

$$T\,F = 1.375$$

and thus the effective Reynolds Number is

$$R\,N_e = 1.375 \times 579{,}000 = 797{,}000$$

The lift coefficient for the desired velocity distribution of Figure 1 is $C_l = 0.21$. The tests of the model were therefore conducted at $C_l = 0.21$ which corresponded to an indicated angle of attack $\alpha = .33^\circ$. Table IX presents the test data and reduction of the data to the velocity distribution and is explained in detail in Appendix I. Figure 11 presents the comparison of the test data with the desired velocity distribution. In general, the agreement is satisfactory except for the region near the trailing edge. In this area the flow is highly turbulent and much of the airstream energy is lost to random rotational motion; thus the region is one of very unstable flow conditions.

DISCUSSION

The method of obtaining the airfoil corresponding to a given velocity distribution as presented in Reference (1) and in this writing is the most direct procedure available to the aerodynamicist. In addition this method undoubtedly yields results of a degree of accuracy satisfactory to most engineering work. Certainly, it presents a solution as accurate as any of the other existing methods, and has the decided advantage that it is much less tedious.

There are, however, several things to be said concerning certain steps in the process. For example, the numerical integration calculations of $\frac{d(\Delta y_t)}{d\,x}$ and $\frac{d\,y_{c_b}}{d\,x}$ involve measurements of the slopes of the curves of $\frac{\Delta v}{V_o}$ and $\frac{{}_oP_b}{4}$ plotted as functions of θ as shown in Figures 3 and 7. Accurate measurements of these slopes is a tedious and difficult task, particularly since in certain areas of these curves, between points from which they were plotted, the shape of the curve is not well defined and hence the slope is questionable. The writer found that the best method of measuring the slopes was by using a thin polished aluminum mirror and adjusting this mirror perpendicular to the curve. This establishes a line perpendicular to the desired slope. The measurements should be done twice, and preferably from opposite approaches to the points in question along the curve.

These numerical integration calculations should, by all means, be made using a good computing machine. A slide rule should not be employed in any phase of the computation.

Another point worthy of special consideration is the adjustment of the original velocity distribution in correcting it to a real velocity distribution. This has previously been discussed in detail.

It should be noted that all curves required by this method should be plotted very accurately on large graph paper. It is now considered by the writer that all the graphs presented herein are much too small. These small curves are very destructive to high degrees of accuracy in evaluating the curves at particular points, and in addition make the mechanical integrations using a planimeter difficult and of questionable accuracy.

And now in considering the comparison of the velocity distribution obtained from the experimental data with the desired velocity distribution as shown in Figure 11, it is to be noted that this comparison does not define the degree of accuracy attainable by this method of finding the airfoil corresponding to a given velocity distribution. The particular calculation presented in this writing, as discussed in the preceding paragraphs, could have been materially improved as regards accuracy in the actual process of calculation. In addition, the airfoil model constructed for testing is certainly subject to slight variations from the true surface defined by the computed ordinates. Moreover, the results of tests conducted in a small wind tunnel of low capacity are not as accurate as may be obtained from more expensive equipment. It is very strongly believed by the writer that a more precise calculation combined with a more perfect airfoil model and high-performance testing facilities would yield experimental data of extremely close agreement to the desired velocity distribution.

RESULTS

The results of the calculation are essentially the ordinates of the derived airfoil. These are plotted in Figure 10 in comparison with the ordinates of the NACA 66(215)-216 airfoil. Now it will be recalled that the original desired velocity distribution as defined by Figure 1 is the theoretical distribution over this NACA configuration Let us, therefore, consider the reasons why the computed airfoil dos not exactly correspond to the NACA 66(215)-216.

First, it is to be noted that the plot of the difference velocity $\frac{\Delta v}{V_o}$ — obtained from the base profile corresponding to the desired velocity distribution and from the selected reference velocity distribution — did not satisfy the requirements that

$$\int_0^{\pi} \frac{\Delta v}{V_o} \, d\theta = 0$$

$$\int_0^{\pi} \frac{\Delta v}{V_o} \times \cos\theta \, d\theta = 0$$

That is, the base profile corresponding to the desired velocity distribution did not correspond to a real base profile having a closed and pointed trailing edge. Therefore, some adjustments were made to the base profile to correct it to a real profile. Had the desired velocity distribution been the true distribution of velocity over the NACA 66(215)-216 airfoil, these adjustments would not have been necessary. The fact that the above requirements were not satisfied indicates that the theoretical distribution chosen as the desired velocity distribution is not the true distribution for the NACA 66(215)-216 airfoil.

Second, the adjustment to the original velocity distribution — made necessary by the changes to the original base profile — was not of a nature such that the general characteristics of the desired velocity distribution were completely retained. And thus the modified velocity distribution for which the corresponding airfoil was derived, no longer conformed exactly with the NACA 66(215)-216 velocity distribution. Therefore, the resulting computed airfoil does not correspond exactly with the NACA 66(215)-216 airfoil.

Consider now the results obtained by the wind-tunnel tests conducted on the model of the derived airfoil. Figure 11 presents the comparison of the experimental velocity distribution and the desired distribution. The comparison over the aft section of the airfoil, particularly with regard to the lower surface velocity distribution, is not as favorable as that over the forward portion of the model. The actual and the desired distributions agree favorably from the leading edge to approximately the 60% chord station. A discussion of the several reasons for the discrepancies in the curves has previously been given. In general, results of the wind-tunnel tests are satisfactory in that the actual velocity distribution is essentially in agreement with the desired distribution of velocity.

The general good agreement of the theory, which neglects viscous effects, with the actual test results indicates that the effects of viscosity are small in this Reynolds Number range. Thus the analysis presented in Reference (1), although based on non-viscous fluid theory, which is never strictly justifiable, yields results of sufficient accuracy for practical engineering purposes.

CONCLUSIONS

The investigation of the Allen airfoil theory presented in this thesis yields the following conclusions with regard to the method defined in Reference (1) of obtaining the airfoil corresponding to a given velocity distribution.

1. The numerical computations involved in the method must be performed with precision. A computing machine is essential.
2. All graphs necessary to the method must be on large sheets. Sizes 8 1/2" by 11" and 11" by 17" are generally unsatisfactory.
3. The effects of viscosity are small in the usual Reynolds Number range.
4. The Allen theory is direct, accurate, and comparatively rapid.

BIBLIOGRAPHY

1. Allen, H. J., "General Theory of Airfoil Sections Having Arbitrary Shape or Pressure Distribution," U. S. National Advisory Committee for Aeronautics Report, No. 833, 1945.

2. Glauert, H., "The Elements of Aerofoil and Airscrew Theory," The University Press (Cambridge), 1926.

3. Theodorsen, Theodore, "On the Theory of Wing Sections with Particular Reference to the Lift Distribution," U. S. National Advisory Committee for Aeronautics Report, No. 383, 1931.

4. Theodorsen, T., and I. E. Garrick, "General Potential Theory of Arbitrary Wing Sections," U. S. National Advisory Committee for Aeronautics Report, No. 452, 1933.

5. Theodorsen, Theodore, "Theory of Wing Sections of Arbitrary Shape," U. S. National Advisory Committee for Aeronautics Report, No. 411, 1931.

6. Abbott, I. A., A. E. Von Doenhoff, and L. S. Stivers, Jr., "Summary of Airfoil Data," U. S. National Advisory Committee for Aeronautics Wartime Report, WRL 560, 1945.

7. Pope, Alan, "Wind Tunnel Testing," John Wiley and Sons, Inc., New York, 1947.

8. Betz, A., "Modification of Wing Section Shape to Assure a Predetermined Change in Pressure Distribution," U. S. National Advisory Committee for Aeronautics Technical Memorandum, No. 767, 1935.

9. Allen, H. Julian, "A Simplified Method for the Calculation of Airfoil Pressure Distribution," U. S. National Advisory Committee for Aeronautics Technical Note, No. 708, 1939.

APPENDIX I

TABLES

TABLE I

CALCULATION OF BASE

PROFILE ORDINATES

(1)	(2)	(3)	(4)	(5)	(6)
$\frac{x}{c}$	$\left(\frac{v}{V_o}\right)_u^2$	$\left(\frac{v}{V_o}\right)_l^2$	$\left(\frac{v}{V_o}\right)_u$	$\left(\frac{v}{V_o}\right)_l$	$\left(\frac{v_l}{V_o} + \frac{v_u}{V_o}\right)$
0	0	0	0	0	0
.025	1.225	.870	1.108	.932	2.040
.050	1.350	1.000	1.162	1.000	2.162
.075	1.400	1.060	1.182	1.030	2.212
.100	1.440	1.100	1.200	1.050	2.250
.150	1.480	1.150	1.217	1.072	2.289
.200	1.520	1.190	1.232	1.090	2.322
.300	1.560	1.230	1.250	1.110	2.360
.400	1.580	1.260	1.258	1.122	2.380
.500	1.600	1.280	1.263	1.130	2.393
.600	1.620	1.300	1.272	1.140	2.412
.700	1.400	1.180	1.182	1.087	2.279
.800	1.130	1.000	1.063	1.000	2.063
.900	.880	.800	.938	.894	1.832
1.000	.615	.620	.784	.784	1.568

(7)	(8)	(9)	(10)	(11)	(12)
$\left(\frac{V_f}{V_o}\right)_1$	$\frac{V_r}{V_o}$	$\left(\frac{\Delta v}{V_o}\right)_1$	θ	$\cos\theta$	$\left(\frac{\Delta v}{V_o}\right)_1 \times \cos\theta$
0	0	0	0	1.0000	0
1.020	1.1226	-.1026	.3176	.9500	-.0974
1.081	1.1946	-.1136	.4510	.9000	-.1020
1.106	1.2151	-.1091	.5548	.8500	-.0926
1.125	1.2206	-.0956	.6435	.8000	-.0765
1.145	1.2154	-.0704	.7954	.7000	-.0493
1.161	1.2019	-.0409	.9273	.6000	-.0256
1.180	1.1668	.0132	1.1593	.4000	.00528
1.190	1.1284	.0616	1.3694	.2000	.0123
1.197	1.0896	.1074	1.5708	0	0
1.204	1.0511	.1529	1.7722	-.2000	-.0306
1.139	1.0135	.1255	1.9823	-.4000	-.0502
1.032	.9769	.0551	2.2143	-.6000	-.0330
.916	.9416	-.0256	2.4981	-.8000	.0205
.784	.9072	-.1232	3.1416	-1.0000	.1232

(13)	(14)	(15)	(16)	(17)
$\left(\frac{\Delta v}{V_o}\right)_2$	$\left(\frac{\Delta v}{V_o}\right)_2 \times \cos\theta$	$\frac{\pi}{2} - \theta$	$(-.000766) \times \left(\frac{\pi}{2} - \theta\right)$	$\Delta\left(\frac{\Delta v}{V_o}\right)$
0	0	1.5708	-.001204	-.0028
-.074	-.0704	1.2532	-.000960	-.0026
-.080	-.0720	1.1198	-.000857	-.0024
-.073	-.0620	1.0160	-.000778	-.0024
-.060	-.0480	.9273	-.000711	-.0023
-.034	-.0238	.7754	-.000594	-.0022
-.009	-.0054	.6435	-.000493	-.0021
.036	.0144	.4115	-.000315	-.0019
.076	.0152	.2014	-.0001542	-.0018
.114	0	0	0	-.0016
.153	-.0306	-.2014	.0001542	-.0014
.126	-.0502	-.4115	.000315	-.0013
.055	-.0330	-.6435	.000493	-.0011
-.030	.0240	-.9273	.000711	-.0009
-.135	.1350	-1.5708	.001204	-.0004

(18)	(19)	(20)	(21)	(22)	(23)
$\frac{\Delta v}{V_o}$	$\frac{\Delta v}{V_o} \cos\theta$	$\frac{V_f}{V_o}$	$\frac{\Delta y_t}{c}$	$\frac{y_r}{c}$	$\frac{y_t}{c}$
0 *	0	0	0	0	0
-.0766	-.0728	1.0460	-.00075	.02786	.02711
-.0824	-.0741	1.1122	-.00132	.03795	.03663
-.0754	-.0640	1.1397	-.00049	.04470	.04421
-.0623	-.0498	1.1583	.00080	.04959	.05039
-.0362	-.0254	1.1792	.00428	.05587	.06015
-.0111	-.0067	1.1908	.00864	.05902	.06766
.0341	.0136	1.2009	.01818	.05936	.07754
.0742	.0148	1.2046	.02700	.05452	.08152
.1124	0	1.2020	.03339	.04649	.07988
.1515	-.03030	1.2026	.03482	.03649	.07131
.1242	-.0496	1.1377	.02860	.02562	.05422
.0540	-.0324	1.0309	.01639	.01491	.03130
-.0309	.0248	.9107	.00174	.00559	.00733
-.1354	.1354	.7718	0	0	0

* The value of $\frac{\Delta v}{V_o}$ is arbitrarily made 0 at $\theta = 0$.

TABLE II

VALUES OF $\frac{\Delta v}{Vo}$ FOR VALUES OF θ
FROM 0 TO 2π, IN $\frac{\pi}{10}$ INCREMENTS
OF θ

Defining $\left(\frac{\Delta v}{Vo}\right)_{\pi + \theta} = \left(\frac{\Delta v}{Vo}\right)_{\pi - \theta}$

θ	$\frac{\Delta v}{Vo}$	θ	$\frac{\Delta v}{Vo}$
0	0	$\frac{11\pi}{10}$	-.111
$\frac{\pi}{10}$	-.076	$\frac{12\pi}{10}$	-.036
$\frac{2\pi}{10}$	-.065	$\frac{13\pi}{10}$	.056
$\frac{3\pi}{10}$	-.009	$\frac{14\pi}{10}$	.139
$\frac{4\pi}{10}$	.052	$\frac{15\pi}{10}$	.113
$\frac{5\pi}{10}$	.113	$\frac{16\pi}{10}$	.052
$\frac{6\pi}{10}$	.139	$\frac{17\pi}{10}$	-.009
$\frac{7\pi}{10}$	.056	$\frac{18\pi}{10}$	-.065
$\frac{8\pi}{10}$	-.036	$\frac{19\pi}{10}$	-.076
$\frac{9\pi}{10}$	-.111	2π	0
π	-.135		

TABLE III

NUMERICAL INTEGRATION CALCULATION OF $\frac{d\Delta y_t}{dx}$

FOR THE BASE PROFILE, WHERE

$$\frac{d\Delta y_t}{dx} = \frac{1}{2\pi}\int_0^{2\pi}\frac{\Delta v}{V_o}\cot\left(\frac{\theta - \theta_o}{2}\right)d\theta$$

(1)	(2)	(3)	(4)	(5)	(6)	(7)
θ Radians	$\frac{x}{c}$	θ Radians	$\frac{\Delta v}{V_o}$	$\frac{d\frac{\Delta v}{V_o}}{d\theta}$	$(a_o)\left(\frac{d\frac{\Delta v}{V_o}}{d\theta}\right)$	$\left(\frac{\Delta v}{V_o}\right)_1$
0	0	0	0	0	0	- -
$\frac{\pi}{10}$	.0244	.314	-.076	-.1644	-.01644	-.065
$\frac{2\pi}{10}$	.0955	.628	-.065	.1578	.01578	-.009
$\frac{3\pi}{10}$	.2061	.941	-.009	.1880	.01880	.052
$\frac{4\pi}{10}$	.3455	1.256	.052	.1868	.01868	.113
$\frac{5\pi}{10}$	.5000	1.570	.113	.1952	.01952	.139
$\frac{6\pi}{10}$	.6545	1.888	.139	-.1231	-.01231	.056
$\frac{7\pi}{10}$	.7939	2.200	.056	-.2836	-.02836	-.036
$\frac{8\pi}{10}$	.9045	2.515	-.036	-.2820	-.02820	-.111
$\frac{9\pi}{10}$	.9756	2.830	-.111	-.1321	-.01321	-.135
π	1.0000	3.142	-.135	-.0358	0	-0.111

(8)	(9)	(10)	(11)	(12)	(13)
$\left(\frac{\Delta v}{V_o}\right)_{-1}$	$\left(\frac{\Delta v}{V_o}\right)_1 - \left(\frac{\Delta v}{V_o}\right)_{-1}$	$a_1\left[\left(\frac{\Delta v}{V_o}\right)_1 - \left(\frac{\Delta v}{V_o}\right)_{-1}\right]$	$\left(\frac{\Delta v}{V_o}\right)_2$	$\left(\frac{\Delta v}{V_o}\right)_{-2}$	$\left(\frac{\Delta v}{V_o}\right)_2 - \left(\frac{\Delta v}{V_o}\right)_{-2}$
- - -	- - -	- - -	- - -	- - -	- - -
0	-.065	-.022575	-.009	.076	-.085
-.076	.067	.023269	.052	0	.052
-.065	.117	.040634	.113	-.076	.189
-.009	.122	.042371	.139	-.065	.204
.052	.087	.030215	.056	-.009	.065
.113	-.057	-.019796	-.036	.052	-.088
.139	-.175	-.060778	-.111	.113	-.224
.056	-.167	-.057999	.135	.139	-.274
-.036	-.099	-.034522	-.111	.056	-.167
-0.111	0	0	-.036	-.036	0

(14)	(15)	(16)	(17)	(18)
$a_2\left[\left(\frac{\Delta v}{Vo}\right)_2 - \left(\frac{\Delta v}{Vo}\right)_{-2}\right]$	$\left(\frac{\Delta v}{Vo}\right)_3$	$\left(\frac{\Delta v}{Vo}\right)_{-3}$	$\left(\frac{\Delta v}{Vo}\right)_3 - \left(\frac{\Delta v}{Vo}\right)_{-3}$	$a_3\left(\frac{\Delta v}{Vo}\right)_3 - \left(\frac{\Delta v}{Vo}\right)_{-3}$
- - -	- - -	- - -	- - -	- - -
-.013362	.052	.065	-.013	-.012948
.008174	.113	.076	.037	.003685
.029711	.139	0	.139	.013844
.032069	.056	-.076	.132	.013147
.010218	-.036	-.065	.029	.002888
-.013834	-.111	-.009	-.102	-.010159
-.035213	-.135	.052	-.187	-.018665
-.043136	-.111	.113	-.224	-.022310
-.026252	-.036	.139	-.175	-.017430
0	.056	.056	0	0

(19)	(20)	(21)	(22)	(23)	(24)
$\left(\frac{\Delta v}{V_o}\right)_4$	$\left(\frac{\Delta v}{V_o}\right)_{-4}$	$\left(\frac{\Delta v}{V_o}\right)_4-\left(\frac{\Delta v}{V_o}\right)_{-4}$	$a_4\left[\left(\frac{\Delta v}{V_o}\right)_4-\left(\frac{\Delta v}{V_o}\right)_{-4}\right]$	$\left(\frac{\Delta v}{V_o}\right)_5$	$\left(\frac{\Delta v}{V_o}\right)_{-5}$
- - -	- - -	- - -	- - -	- - -	- - -
.113	.009	.104	.007186	.139	-.052
.139	.065	.074	.005113	.056	.009
.056	.076	-.020	.001382	-.036	.065
-.036	0	-.036	-.002488	-.111	.076
-.111	-.076	-.035	-.002419	-.135	0
-.135	-.065	-.070	-.004865	-.111	-.076
-.111	-.009	-.102	-.007048	-.036	-.065
-.036	.052	-.088	-.006081	.056	-.009
.056	.113	-.057	-.003939	.139	.052
.139	.139	0	0	.113	.113

(25)	(26)	(27)	(28)	(29)
$\left(\frac{\Delta v}{V_o}\right)_5 - \left(\frac{\Delta v}{V_o}\right)_{-5}$	$a_5\left[\left(\frac{\Delta v}{V_o}\right)_5 - \left(\frac{\Delta v}{V_o}\right)_{-5}\right]$	$\left(\frac{\Delta v}{V_o}\right)_6$	$\left(\frac{\Delta v}{V_o}\right)_{-6}$	$\left(\frac{\Delta v}{V_o}\right)_6 - \left(\frac{\Delta v}{V_o}\right)_{-6}$
- - -	- - -	- - -	- - -	- - -
.191	.009607	.056	-.113	.169
.047	.002364	-.036	-.052	.016
-.101	-.005080	-.111	.009	-.120
-.187	-.009406	-.135	.065	-.200
-.135	-.006811	-.111	.076	-.187
-.035	-.001761	-.036	0	-.036
.029	.001458	.056	-.076	.132
.065	.003270	.139	-.065	.204
.087	.004376	.113	-.009	.122
0	0	.052	.052	0

(30)	(31)	(32)	(33)	(34)
$a_6\left[\left(\frac{\Delta v}{V_o}\right)_6 - \left(\frac{\Delta v}{V_o}\right)_{-6}\right]$	$\left(\frac{\Delta v}{V_o}\right)_7$	$\left(\frac{\Delta v}{V_o}\right)_{-7}$	$\left(\frac{\Delta v}{V_o}\right)_7 - \left(\frac{\Delta v}{V_o}\right)_{-7}$	$a_7\left[\left(\frac{\Delta v}{V_o}\right)_7 - \left(\frac{\Delta v}{V_o}\right)_{-7}\right]$
- - -	- - -	- - -	- - -	- - -
.006185	-.036	-.139	.103	.002894
.000586	-.111	-.113	.002	.000056
-.004392	-.135	-.052	-.083	-.002330
-.007335	-.111	.009	-.120	-.003372
-.006844	-.036	.065	-.101	-.002838
-.001318	.056	.076	-.020	-.005620
.004831	.139	0	.139	.003906
.007466	.113	-.076	.189	.005311
.004465	.052	-.065	.117	.003288
0	-.009	-.009	0	0

(35)	(36)	(37)	(38)	(39)
$\left(\frac{\Delta v}{V_o}\right)_8$	$\left(\frac{\Delta v}{V_o}\right)_{-8}$	$\left(\frac{\Delta v}{V_o}\right)_8 - \left(\frac{\Delta v}{V_o}\right)_{-8}$	$a_8\left[\left(\frac{\Delta v}{V_o}\right)_8 - \left(\frac{\Delta v}{V_o}\right)_{-8}\right]$	$\left(\frac{\Delta v}{V_o}\right)_9$
- - -	- - -	- - -	- - -	- - -
-.111	-.056	-.055	-.000897	-.135
-.135	-.139	.004	.000059	-.111
-.111	-.113	.002	.000033	-.036
-.036	-.052	.088	.001434	.056
.056	.009	.047	.000766	.139
.139	.065	.074	.001206	.113
.113	.076	.037	.000603	.052
.052	0	.052	.000848	-.009
-.009	-.076	.067	.001092	-.065
-.065	-.065	0	0	-.076

(40)	(41)	(42)	(43)
$\left(\frac{\Delta v}{V_o}\right)_{-9}$	$\left(\frac{\Delta v}{V_o}\right)_9 - \left(\frac{\Delta v}{V_o}\right)_{-9}$	$a_9\left[\left(\frac{\Delta v}{V_o}\right)_9 - \left(\frac{\Delta v}{V_o}\right)_{-9}\right]$	$\frac{d\,\Delta y_t}{d\,x}$
- - -	- - -	- - -	0 *
.036	-.171	-.001371	-.04172
-.056	-.055	-.000440	.05865
-.139	.103	.000824	.09343
-.113	.169	.001352	.08645
-.052	.191	.001528	.04622
.009	.104	.000832	-.06762
.065	-.013	-.000104	-.13937
.076	-.085	-.000680	-.14151
0	-.065	-.000520	-.08265
-.076	0	0	0

* The value of $\frac{d\,\Delta y_t}{dx} = 0$ at $\theta_o = 0$
by inspection of equation (40).

TABLE IV

FINAL ADJUSTMENT OF THE DESIRED VELOCITY DISTRIBUTION, AND CALCULATION OF THE BASIC PRESSURE DISTRIBUTION

(1)	(2)	(3)	(4)	(5)
$\frac{x}{c}$	$\frac{v_u}{V_o} - \frac{V_f}{V_o}$	$\frac{P_b}{4}$	$\frac{P_b/4}{V_f/V_o}$	$\frac{v_1}{V_o}$
0	0	0	0	0
.025	.062	.0655	.062	.9840
.050	.050	.0556	.050	1.0622
.075	.042	.0478	.042	1.0977
.100	.042	.0486	.042	1.1163
.150	.038	.0447	.038	1.1412
.200	.041	.0487	.041	1.1498
.300	.049	.0587	.049	1.1519
.400	.053	.0639	.053	1.1516
.500	.061	.0733	.061	1.1410
.600	.069	.0830	.069	1.1336
.700	.044	.0500	.044	1.0937
.800	.032	.0330	.032	.9989
.900	.027	.0249	.027	.8834
1.000	0	0	0	.7718

TABLE V

CALCULATION OF MEAN CAMBER

LINE ORDINATES

(1)	(2)	(3)	(4)	(5)
$\frac{x}{c}$	$\frac{V_u}{V_o} - \frac{V_l}{V_o}$	${}_oP_b$	$\frac{{}_oP_b}{4}$	θ
0	0	0	0	0
.025	.1240	.2480	.0620	.3176
.050	.0998	.1996	.0499	.4510
.075	.0843	.1686	.0422	.5548
.100	.0837	.1674	.0419	.6435
.150	.0758	.1516	.0379	.7954
.200	.0822	.1644	.0411	.9273
.300	.0981	.1962	.0491	1.1593
.400	.1064	.2128	.0532	1.3694
.500	.1220	.2440	.0610	1.5708
.600	.1364	.2728	.0682	1.7722
.700	.0880	.1760	.0440	1.9823
.800	.0640	.1280	.0320	2.2143
.900	.0550	.1100	.0275	2.4981
1.000	0	0	0	3.1416

(6)	(7)	(8)	(9)	(10)
$\frac{V_f}{V_o}$	P_b	$\frac{y_{c_b}}{c}$	$\frac{x}{c}\alpha_i$	$\frac{y_c}{c}$
1.0460	.2620	.00178	.00011	.00189
1.1122	.2224	.00288	.00021	.00309
1.1397	.1910	.00390	.00032	.00422
1.1583	.1942	.00466	.00042	.00508
1.1792	.1790	.00600	.00069	.00669
1.1908	.1950	.00736	.00085	.00821
1.2009	.2350	.00980	.00127	.01107
1.2046	.2580	.01148	.00170	.01318
1.2020	.2932	.01216	.00212	.01428
1.2026	.3320	.01164	.00255	.01419
1.1377	.2000	.00846	.00297	.01143
1.0309	.1320	.00324	.00339	.00663
.9107	.0995	.00052	.00382	.00434
.7718	0	-.00424	.00424	0

TABLE VI

VALUES OF $\frac{{}_oP_b}{4}$ FOR VALUES OF θ
FROM 0 TO 2π, IN $\frac{\pi}{10}$ INCREMENTS
OF θ

Defining $\left(\frac{{}_oP_b}{4}\right)_{\pi+\theta} = -\left(\frac{{}_oP_b}{4}\right)_{\pi-\theta}$

θ	$\frac{{}_oP_b}{4}$	θ	$\frac{{}_oP_b}{4}$
0	0	$\frac{11\pi}{10}$	-.0113
$\frac{\pi}{10}$	.0620	$\frac{12\pi}{10}$	-.0268
$\frac{2\pi}{10}$	.0417	$\frac{13\pi}{10}$	-.0326
$\frac{3\pi}{10}$	.0416	$\frac{14\pi}{10}$	-.0584
$\frac{4\pi}{10}$	.0510	$\frac{15\pi}{10}$	-.0610
$\frac{5\pi}{10}$	.0610	$\frac{16\pi}{10}$	-.0510
$\frac{6\pi}{10}$	.0584	$\frac{17\pi}{10}$	-.0416
$\frac{7\pi}{10}$	.0326	$\frac{18\pi}{10}$	-.0417
$\frac{8\pi}{10}$	.0268	$\frac{19\pi}{10}$	-.0620
$\frac{9\pi}{10}$	.0113	2π	0
π	0		

TABLE VII

NUMERICAL INTEGRATION CALCULATION OF $\frac{d\, y_{c_b}}{d\, x}$

FOR MEAN CAMBER LINE, WHERE

$$\frac{d\, y_{c_b}}{d\, x} = \frac{1}{2\pi}\int_0^{2\pi} \frac{{}_oP_b}{4} \operatorname{Cot}\left(\frac{\theta - \theta_o}{2}\right) d\,\theta$$

(1) θ Radians	(2) $\frac{x}{c}$	(3) θ Radians	(4) $\frac{{}_oP_b}{4}$	(5) $\frac{d\left(\frac{{}_oP_b}{4}\right)}{d\,\theta}$	(6) $a_o\left[\frac{d\left(\frac{{}_oP_b}{4}\right)}{d\,\theta}\right]$	(7) $\left(\frac{{}_oP_b}{4}\right)_1$
0	0	0	0	0	0	.062
$\frac{\pi}{10}$	.0244	.314	.0620	-.0750	-.00750	.0417
$\frac{2\pi}{10}$	.0955	.628	.0417	-.0044	-.00044	.0416
$\frac{3\pi}{10}$	.2061	.941	.0416	.0427	.00427	.0510
$\frac{4\pi}{10}$	.3455	1.256	.0510	.0182	.00182	.0610
$\frac{5\pi}{10}$	.5000	1.570	.0610	.0403	.00403	.0584
$\frac{6\pi}{10}$	.6545	1.888	.0584	-.1053	-.01053	.0326
$\frac{7\pi}{10}$	.7939	2.200	.0326	-.0325	-.00325	.0268
$\frac{8\pi}{10}$	.9045	2.515	.0268	-.0285	-.00285	.0113
$\frac{9\pi}{10}$	.9756	2.830	.0113	-.0625	-.00625	0
π	1.0000	3.142	0	0	0	-.0113

(8)	(9)	(10)	(11)	(12)
$\left(\frac{{}_oP_b}{4}\right)_{-1}$	$\left(\frac{{}_oP_b}{4}\right)_1 - \left(\frac{{}_oP_b}{4}\right)_{-1}$	$a_1\left[\left(\frac{{}_oP_b}{4}\right)_1 - \left(\frac{{}_oP_b}{4}\right)_{-1}\right]$	$\left(\frac{{}_oP_b}{4}\right)_2$	$\left(\frac{{}_oP_b}{4}\right)_{-2}$
-.0620	.1240	.043065	.0417	-.0417
0	.0417	.014482	.0416	-.0620
.0620	-.0204	-.007085	.0510	0
.0417	.0093	.003230	.0610	.0620
.0416	.0194	.006738	.0584	.0417
.0510	.0074	.002570	.0326	.0416
.0610	-.0284	-.009863	.0268	.0510
.0584	-.0316	-.010975	.0113	.0610
.0326	-.0213	-.007397	0	.0584
.0268	-.0268	-.009308	-.0113	.0326
.0113	-.0226	-.007849	-.0268	.0268

(13)	(14)	(15)	(16)	(17)
$\left(\frac{{}_oP_b}{4}\right)_2-\left(\frac{{}_oP_b}{4}\right)_{-2}$	$a_2\left[\left(\frac{{}_oP_b}{4}\right)_2-\left(\frac{{}_oP_b}{4}\right)_{-2}\right]$	$\left(\frac{{}_oP_b}{4}\right)_3$	$\left(\frac{{}_oP_b}{4}\right)_{-3}$	$\left(\frac{{}_oP_b}{4}\right)_3-\left(\frac{{}_oP_b}{4}\right)_{-3}$
.0834	.013110	.0416	-.0416	.0832
.1036	.016286	.0510	-.0417	.0927
.0510	.008017	.0610	-.0620	.1230
-.0010	-.000157	.0584	0	.0584
.0167	.002625	.0326	.0620	-.0294
-.0090	-.001415	.0268	.0417	-.0149
-.0242	-.003804	.0113	.0416	-.0303
-.0497	-.007813	0	.0510	-.0510
-.0584	-.009180	-.0113	.0610	-.0723
-.0439	-.006901	-.0268	.0584	-.0852
-.0536	-.008426	-.0326	.0326	-.0652

(18)	(19)	(20)	(21)	(22)
$a_3\left[\left(\frac{{}_oP_b}{4}\right)_3-\left(\frac{{}_oP_b}{4}\right)_{-3}\right]$	$\left(\frac{{}_oP_b}{4}\right)_4$	$\left(\frac{{}_oP_b}{4}\right)_{-4}$	$\left(\frac{{}_oP_b}{4}\right)_4-\left(\frac{{}_oP_b}{4}\right)_{-4}$	$a_4\left[\left(\frac{{}_oP_b}{4}\right)_4-\left(\frac{{}_oP_b}{4}\right)_{-4}\right]$
.008287	.0510	-.0510	.1020	.007048
.009233	.0610	-.0416	.1026	.007090
.012251	.0584	-.0417	.1001	.006917
.005817	.0326	-.0620	.0946	.006537
-.002928	.0268	0	.0268	.001852
-.001484	.0113	.0620	-.0507	-.003503
-.003018	0	.0417	-.0417	-.002881
-.005080	-.0113	.0416	-.0529	-.003655
-.007201	-.0268	.0510	-.0778	-.005376
-.008486	-.0326	.0610	-.0936	-.006468
-.006494	-.0584	.0584	-.1168	-.008071

(23)	(24)	(25)	(26)	(27)
$\left(\frac{{}_oP_b}{4}\right)_5$	$\left(\frac{{}_oP_b}{4}\right)_{-5}$	$\left(\frac{{}_oP_b}{4}\right)_5 - \left(\frac{{}_oP_b}{4}\right)_{-5}$	$a_5\left[\left(\frac{{}_oP_b}{4}\right)_5 - \left(\frac{{}_oP_b}{4}\right)_{-5}\right]$	$\left(\frac{{}_oP_b}{4}\right)_6$
.0610	-.0610	.1220	.006137	.0584
.0584	-.0510	.1094	.005503	.0326
.0326	-.0416	.0742	.003732	.0268
.0268	-.0417	.0685	.003446	.0113
.0113	-.0620	.0733	.003687	0
0	0	0	0	-.0113
-.0113	.0620	-.0733	-.003687	-.0268
-.0268	.0417	-.0685	-.003446	-.0326
-.0326	.0416	-.0742	-.003732	-.0584
-.0584	.0510	-.1094	-.005503	-.0610
-.0610	.0610	-.1220	-.006137	-.0510

(28)	(29)	(30)	(31)	(32)
$\left(\frac{oP_b}{4}\right)_{-6}$	$\left(\frac{oP_b}{4}\right)_6 - \left(\frac{oP_b}{4}\right)_{-6}$	$a_6\left[\left(\frac{oP_b}{4}\right)_6 - \left(\frac{oP_b}{4}\right)_{-6}\right]$	$\left(\frac{oP_b}{4}\right)_7$	$\left(\frac{oP_b}{4}\right)_{-7}$
-.0584	.1168	.004275	.0326	-.0326
-.0610	.0936	.003426	.0268	-.0584
-.0510	.0778	.002847	.0113	-.0610
-.0416	.0529	.001936	0	-.0510
-.0417	.0417	.001526	-.0113	-.0416
-.0620	.0507	.001856	-.0268	-.0417
0	-.0268	-.000981	-.0326	-.0620
.0620	-.0946	-.003462	-.0584	0
.0417	-.1001	-.003664	-.0610	.0620
.0416	-.1026	-.003755	-.0510	.0417
.0510	-.1020	-.003733	-.0416	.0416

(33)	(34)	(35)	(36)	(37)
$\left(\frac{{}_oP_b}{4}\right)_7 - \left(\frac{{}_oP_b}{4}\right)_{-7}$	$a_7\left[\left(\frac{{}_oP_b}{4}\right)_7 - \left(\frac{{}_oP_b}{4}\right)_{-7}\right]$	$\left(\frac{{}_oP_b}{4}\right)_8$	$\left(\frac{{}_oP_b}{4}\right)_{-8}$	$\left(\frac{{}_oP_b}{4}\right)_8 - \left(\frac{{}_oP_b}{4}\right)_{-8}$
.0652	.001832	.0268	-.0268	.0536
.0852	.002394	.0113	-.0326	.0439
.0723	.002032	0	-.0584	.0584
.0510	.001433	-.0113	-.0610	.0497
.0303	.000851	-.0268	-.0510	.0242
.0149	.000419	-.0326	-.0416	.0090
.0294	.000826	-.0584	-.0417	-.0167
-.0584	-.001641	-.0610	-.0620	.0010
-.1230	-.003456	-.0510	0	-.0510
-.0927	-.002605	-.0416	.0620	-.1036
-.0832	-.002338	-.0417	.0417	-.0834

(38)	(39)	(40)	(41)
$a_8\left[\left(\frac{{}_oP_b}{4}\right)_8 - \left(\frac{{}_oP_b}{4}\right)_{-8}\right]$	$\left(\frac{{}_oP_b}{4}\right)_9$	$\left(\frac{{}_oP_b}{4}\right)_{-9}$	$\left(\frac{{}_oP_b}{4}\right)_9 - \left(\frac{{}_oP_b}{4}\right)_{-9}$
.000874	.0113	-.0113	.0226
.000716	0	-.0268	.0268
.000952	-.0113	-.0326	.0213
.000810	-.0268	-.0584	.0316
.000394	-.0326	-.0610	.0284
.000147	-.0584	-.0510	-.0074
-.000272	-.0610	-.0416	-.0194
.000016	-.0510	-.0417	-.0093
-.000831	-.0416	-.0620	.0204
-.001689	-.0417	0	-.0417
-.001359	-.0620	.0620	-.1240

(42)	(43)
$a_9\left[\left(\frac{{}_oP_b}{4}\right)_9-\left(\frac{{}_oP_b}{4}\right)_{-9}\right]$	$\frac{d\,{}^{y}c_b}{d\,x}$
.000181	.08481
.000214	.05184
.000170	.02940
.000253	.02757
.000227	.01679
-.000059	.00256
-.000155	-.03436
-.000074	-.03938
.000163	-.04353
-.000334	-.05130
-.000992	-.04540

TABLE VIII

CALCULATION OF AIRFOIL ORDINATES

(1) $\frac{x}{c}$	(2) $\frac{d\, y_{c_b}}{d\, x}$	(3) $\frac{d\, y_c}{d\, x}$	(4) β Radians	(5) $\sin\beta$	(6) $\cos\beta$	(7) $\frac{y_t}{c}$
0	.0850	.0892	.0892	.0892	.9960	0
.025	.0518	.0560	.0560	.0560	.9984	.0271
.050	.0414	.0456	.0456	.0456	.9990	.0366
.075	.0343	.0385	.0385	.0385	.9993	.0442
.100	.0290	.0332	.0332	.0332	.9995	.0504
.150	.0280	.0322	.0322	.0322	1.0000	.0602
.200	.0274	.0316	.0316	.0316	1.0000	.0677
.300	.0208	.0250	.0250	.0250	1.0000	.0775
.400	.0120	.0162	.0162	.0162	1.0000	.0815
.500	.0026	.0068	.0068	.0068	1.0000	.0799
.600	-.0200	-.0158	-.0158	-.0158	1.0000	.0713
.700	-.0376	-.0334	-.0334	-.0334	1.0000	.0542
.800	-.0396	-.0354	-.0354	-.0354	1.0000	.0313
.900	-.0431	-.0389	-.0389	-.0389	1.0000	.0073
1.000	-.0450	-.0408	-.0408	-.0408	1.0000	0

(8)	(9)	(10)	(11)	(12)	(13)	(14)
$\frac{y_t \sin\beta}{c}$	$\frac{y_t \cos\beta}{c}$	$\frac{y_c}{c}$	$\frac{x_u}{c}$	$\frac{y_u}{c}$	$\frac{x_l}{c}$	$\frac{y_l}{c}$
0	0	0	0	0	0	0
.0015	.0271	.0019	.0235	.0290	.0265	-.0252
.0017	.0366	.0031	.0483	.0397	.0517	-.0335
.0017	.0442	.0042	.0733	.0484	.0767	-.0400
.0017	.0504	.0051	.0983	.0555	.1017	-.0453
.0019	.0601	.0067	.1481	.0668	.1519	-.0534
.0021	.0677	.0082	.1979	.0759	.2021	-.0595
.0019	.0775	.0111	.2981	.0886	.3019	-.0664
.0013	.0815	.0132	.3987	.0947	.4013	-.0683
.0005	.0799	.0143	.4995	.0942	.5005	-.0656
.0011	.0713	.0142	.5989	.0855	.6011	-.0571
.0018	.0542	.0114	.6982	.0656	.7018	-.0428
.0011	.0313	.0066	.7989	.0379	.8011	-.0247
.0003	.0073	.0043	.8997	.0116	.9003	-.0030
0	0	0	1.0000	0	1.0000	0

TABLE IX

EXPERIMENTAL DATA AND DETERMINATION OF THE ACTUAL VELOCITY DISTRIBUTION FOR MODEL OF CALCULATED AIRFOIL TESTED IN THE LOW-SPEED WIND-TUNNEL AT THE GEORGIA INSTITUTE OF TECHNOLOGY

(1)	(2)	(3)	(4)	(5)
$\frac{x}{c}$	P_u Centimeters of Alcohol	ΔP_u Centimeters of Alcohol	$\frac{\Delta P_u}{q}$	$\frac{v_u^2}{V_o^2}$
0	-7.43	10.00	.996	.004
.025	3.93	-1.36	-.136	1.136
.050	5.49	-2.92	-.291	1.291
.075	5.84	-3.27	-.326	1.326
.100	6.48	-3.91	-.390	1.390
.150	6.96	-4.39	-.437	1.437
.200	8.11	-5.54	-.552	1.552
.300	8.57	-6.00	-.597	1.597
.400	8.89	-6.32	-.630	1.630
.500	8.85	-6.28	-.626	1.626
.600	7.91	-5.34	-.532	1.532
.650	7.06	-4.49	-.447	1.447
.700	5.66	-2.99	-.298	1.298
.800	2.91	- .34	-.034	1.034
.900	1.49	1.08	.108	.892
1.000	.096	2.47	.246	.754

(6) P_1 Centimeters of Alcohol	(7) ΔP_1 Centimeters of Alcohol	(8) $\frac{\Delta P_1}{q}$	(9) $\frac{v_1^2}{V_o^2}$
-7.43	10.00	.996	.004
2.27	.30	.030	.970
3.69	-1.12	-.112	1.112
4.20	-1.63	-.162	1.162
4.56	-1.99	-.198	1.198
5.66	-3.09	-.308	1.308
6.02	-3.45	-.344	1.344
5.70	-3.13	-.312	1.312
5.92	-3.35	-.334	1.334
5.74	-3.17	-.316	1.316
5.22	-2.65	-.264	1.264
4.38	-1.81	-.180	1.180
3.42	- .85	-.085	1.085
2.01	.56	.056	.944
---	---	---	---
.096	2.47	.246	.754

EXPLANATION OF TABLES

TABLE I

Column	Remarks
(1)	Chordwise station
(2)	Desired upper surface velocity distribution, Figure 1
(3)	Desired lower surface velocity distribution, Figure 1
(4)	$\sqrt{(2)}$
(5)	$\sqrt{(3)}$
(6)	(4) + (5)
(7)	$\frac{(6)}{2}$ Base profile velocity distribution, 1st choice, Figure 2
(8)	Reference base profile velocity distribution, Reference (1)
(9)	(7) - (8), Figure 3, uncorrected $\frac{\Delta v}{V_o}$
(10)	θ
(11)	Cos θ
(12)	(9)(11)
(13)	First adjustment of $\frac{\Delta v}{V_o}$, Figure 3
(14)	(13)(11)
(15)	$\pi/2$ - (10) Reference (1). Method for final correction to $\frac{\Delta v}{V_o}$
(16)	-.000766 x (15), Reference (1). Method for final correction to $\frac{\Delta v}{V_o}$
(17)	$\Delta\left(\frac{\Delta v}{V_o}\right)$, -.00166 + (16), " " " " " " " "
(18)	(13) + (17), Corrected $\frac{\Delta v}{V_o}$. Figure 3 *
(19)	(18)(11)
(20)	(8) + (18)
(21)	Mechanical integration of Figure 4

(22) Ordinates for reference base profile, Reference (1)

(23) (21) - (22), Ordinates of base profile

* It is to be noted that the value of $\Delta v/V_o$ is arbitrarily made 0 at $\theta = 0$.

TABLE II

Column	Remarks
θ	The values of $\frac{\Delta v}{V_o}$ are taken from Figure 3. The values of $\frac{\Delta v}{V_o}$ for values of θ greater than π are obtained from the definition $\left(\frac{\Delta v}{V_o}\right)_{\pi+\theta} = \left(\frac{\Delta v}{V_o}\right)_{\pi-\theta}$

TABLE III

Column	Remarks
(1)	θ
(2)	Chordwise station
(3)	θ
(4)	Table II
(5)	Slope as measured from Figure 3
(6)	$a_o(5)$, where $a_o = .1000$
(7)	$\frac{\Delta v}{V_o}$ at $\theta_o + \frac{n\pi}{10}$, where $n = 1$; Table II. Note: The value of $d\Delta y_t/dx$ = zero at $\theta_o = 0$ by inspection of Equation (40).
(8)	$\frac{\Delta v}{V_o}$ at $\theta_o + \frac{n\pi}{10}$, where $n = -1$; Table II. Note: The value of $d\Delta y_t/dx$ = zero at $\theta_o = 0$ by inspection of Equation (40).
(9)	(7) - (8)
(10)	$a_1(9)$, where $a_1 = .3473$
(11)$\rightarrow$(42)	Similar to (7) $\rightarrow$ (11), n = 2,-2, ...9,-9
(43)	(6) + (10) + (14) + (18) + (22) + (26) + (30) + (34) + (38) + (42)

TABLE IV

Column	Remarks
(1)	Chordwise station
(2)	[(4) - (20)], Table I
(3)	[(20), Table I] x (2)
(4)	(3) ÷ [(20), Table I]
(5)	[(20), Table I] - (4)

TABLE V

Column	Remarks
(1)	Chordwise station
(2)	[(4), Table I] - [(5), Table IV]
(3)	2(2), Basic pressure distribution, zero profile thickness
(4)	(3)/4
(5)	θ
(6)	[(20), Table I]
(7)	(3)(6), Basic pressure distribution
(8)	Mean camber line ordinates, uncorrected for α_i, obtained by mechanical integration of Figure 8
(9)	(α_i)(1), where α_i = .00424 radians
(10)	(8) + (9), Corrected mean camber line ordinates

TABLE VI

Column	Remarks
(1)	The values of $\frac{{}_oP_b}{4}$ are taken from Figure 7. The values of $\frac{{}_oP_b}{4}$ for values of θ greater than π are obtained from the definition $\left(\frac{{}_oP_b}{4}\right)_{\pi+\theta} = -\left(\frac{{}_oP_b}{4}\right)_{\pi-\theta}$.

TABLE VII

Column	Remarks
(1)	θ
(2)	Chordwise station
(3)	θ
(4)	Table VI
(5)	Slope as measured from Figure 7
(6)	a_o (5), where a_o = .1000
(7)	$\frac{{}_oP_b}{4}$ at $\theta_o + \frac{n\pi}{10}$ where n = 1, Table VI
(8)	$\frac{{}_oP_b}{4}$ at $\theta_o + \frac{n\pi}{10}$ where n = -1, Table VI
(9)	(7) - (8)
(10)	a_1 (9) where a_1 = .3473
(11)→(42)	Similar to (7)→(11), n = 2, -2, ... 9, -9.
(43)	(6) + (10) + (14) + (18) + (22) + (26) + (30) + (34) + (38) + (42)

TABLE VIII

Column	Remarks
(1)	Chordwise station
(2)	Figure 8
(3)	(2) + α_i, where α_i = .00424
(4)	$\tan^{-1}$ (3), For small angles tangent β = angle β
(5)	Sin (4), For small angles, the sine β = angle β
(6)	Cos (4)
(7)	(23), Table I
(8)	(7)(5)
(9)	(7)(6)
(10)	(10), Table V
(11)	(1) - (8)
(12)	(9) + (10)
(13)	(1) + (8)
(14)	(10) - (9)

TABLE IX

Column	Remarks
(1)	Chordwise station
(2)	Experimental data, wind tunnel
(3)	Static pressure in tunnel test section - (2), where p_s = 2.57 centimeters of alcohol
(4)	(3) ÷ q, where q = 10.03 centimeters of alcohol
(5)	1.000 - (4)
(6)	Experimental data, wind tunnel
(7)	Static pressure in tunnel test section - (6)
(8)	(7) ÷ q, where q = 10.03 centimeters of alcohol
(9)	1.000 - (8)

APPENDIX II

FIGURES

FIGURE 1

DESIRED VELOCITY DISTRIBUTION

(NACA 66(215)-216)

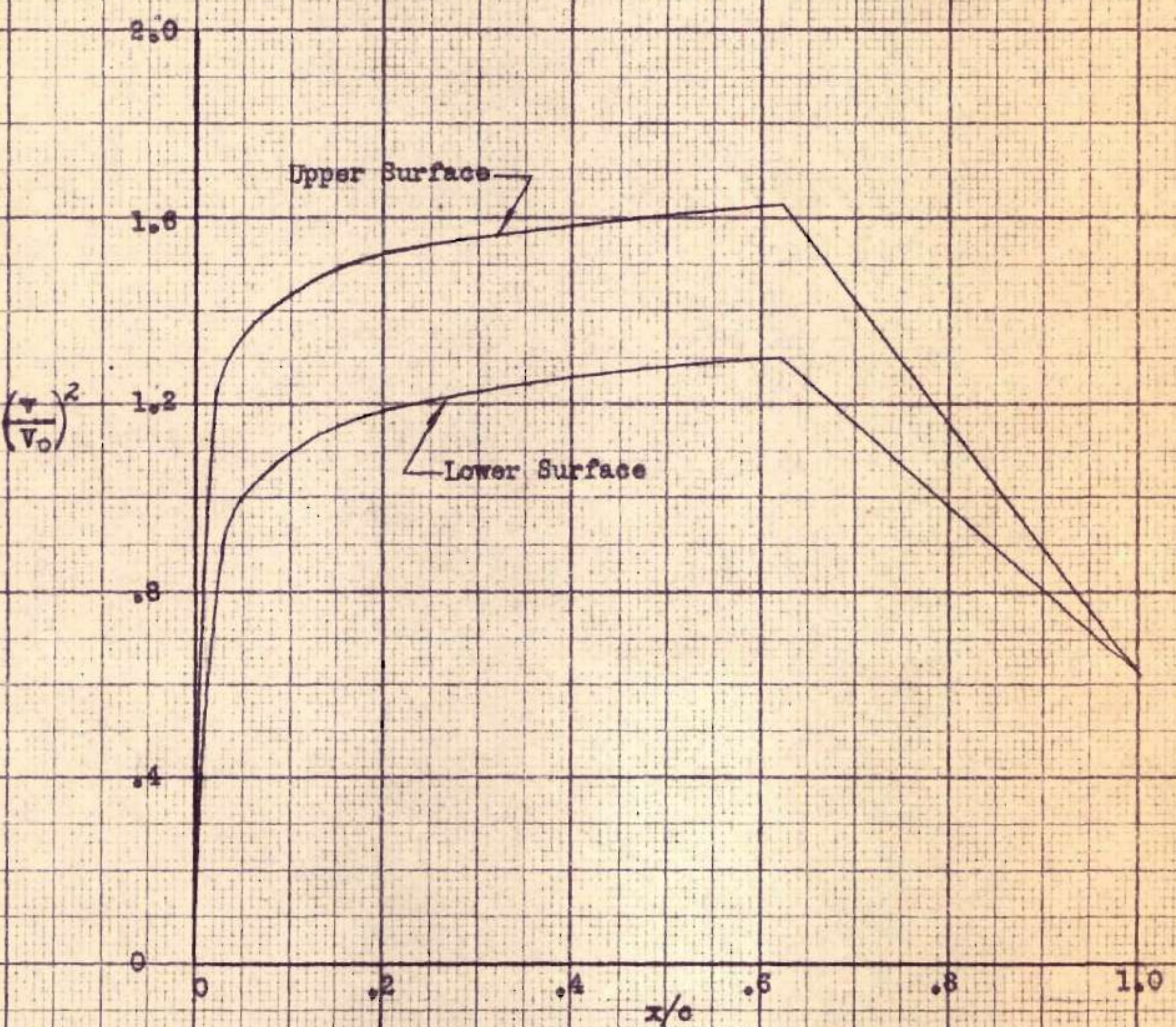

FIGURE 2

DESIRED VELOCITY DISTRIBUTION, BASE PROFILE VELOCITY DISTRIBUTION, NACA 66_4-021 UPPER SURFACE DISTRIBUTION AND NACA 66,1-012 LOWER SURFACE DISTRIBUTION

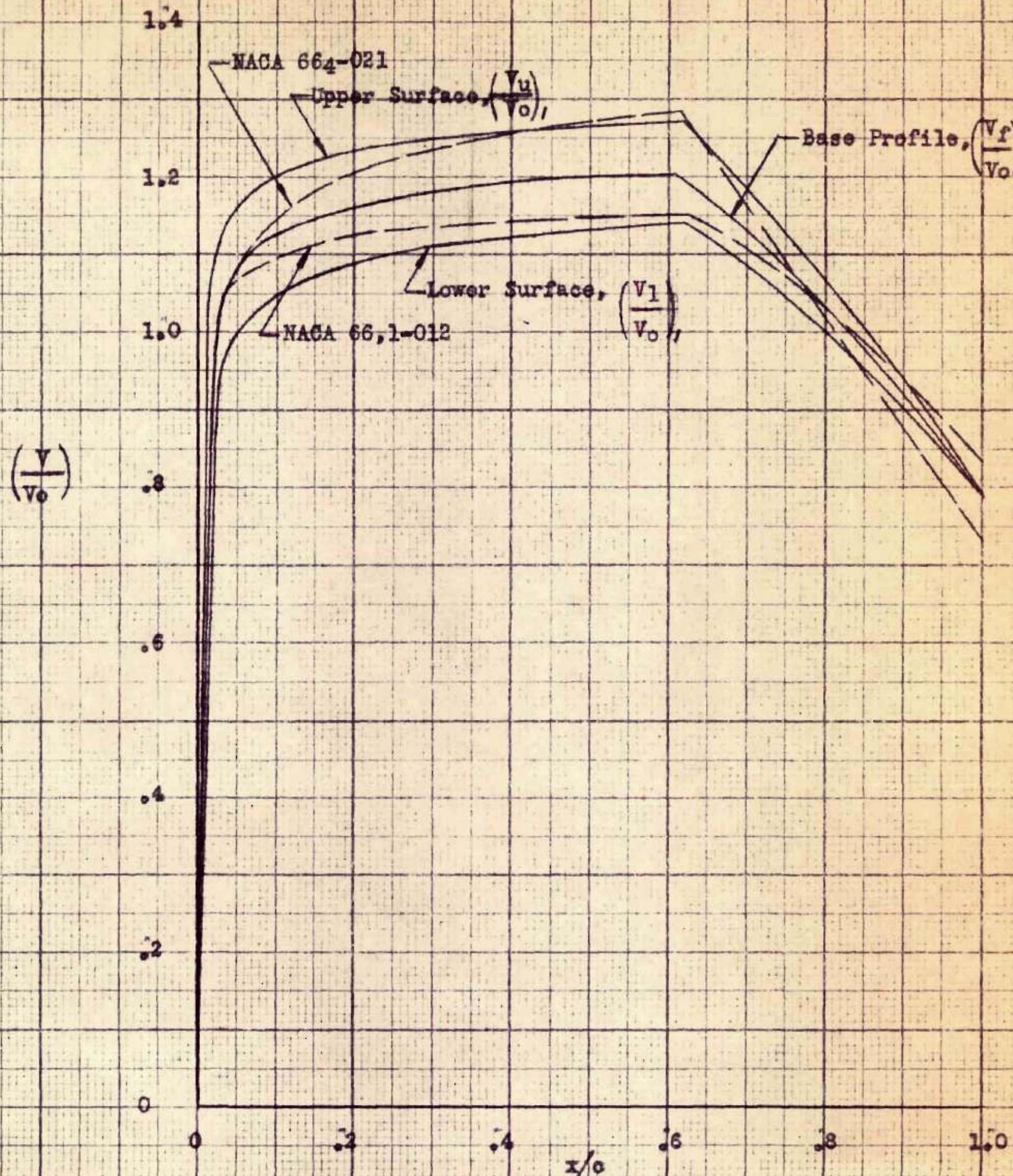

FIGURE 3

$\frac{\Delta v}{V_o}$ AND $\frac{\Delta v}{V_o}$ Cos θ VERSUS θ

ADJUSTMENT OF BASE PROFILE DIFFERENCE VELOCITY DISTRIBUTION

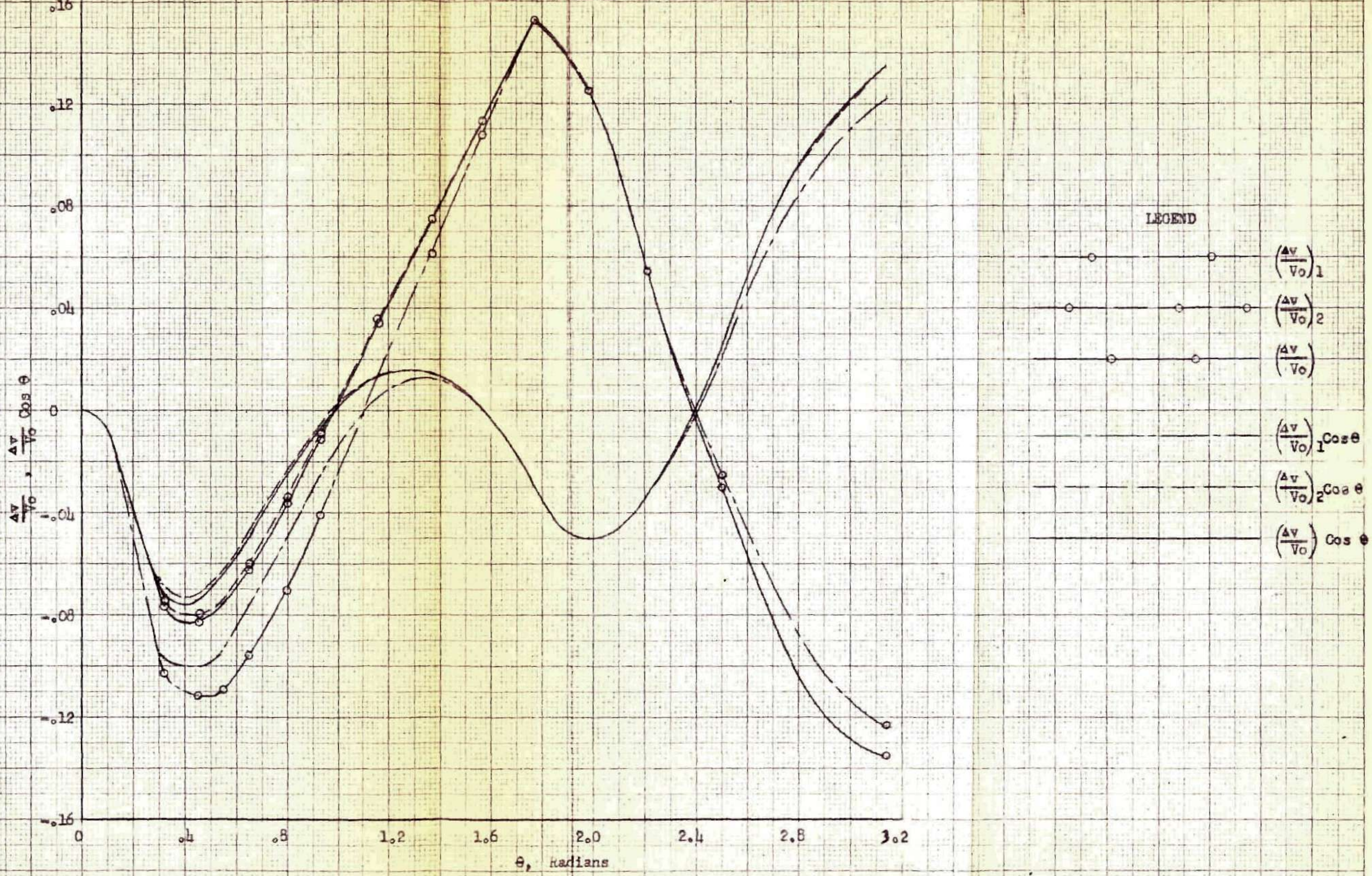

FIGURE 4

$\frac{d\Delta y_t}{dx}$ PLOTTED AS A FUNCTION OF x/c. MECHANICAL INTEGRATION OF THIS CURVE YIELDS VALUES OF $\frac{\Delta y_t}{c}$

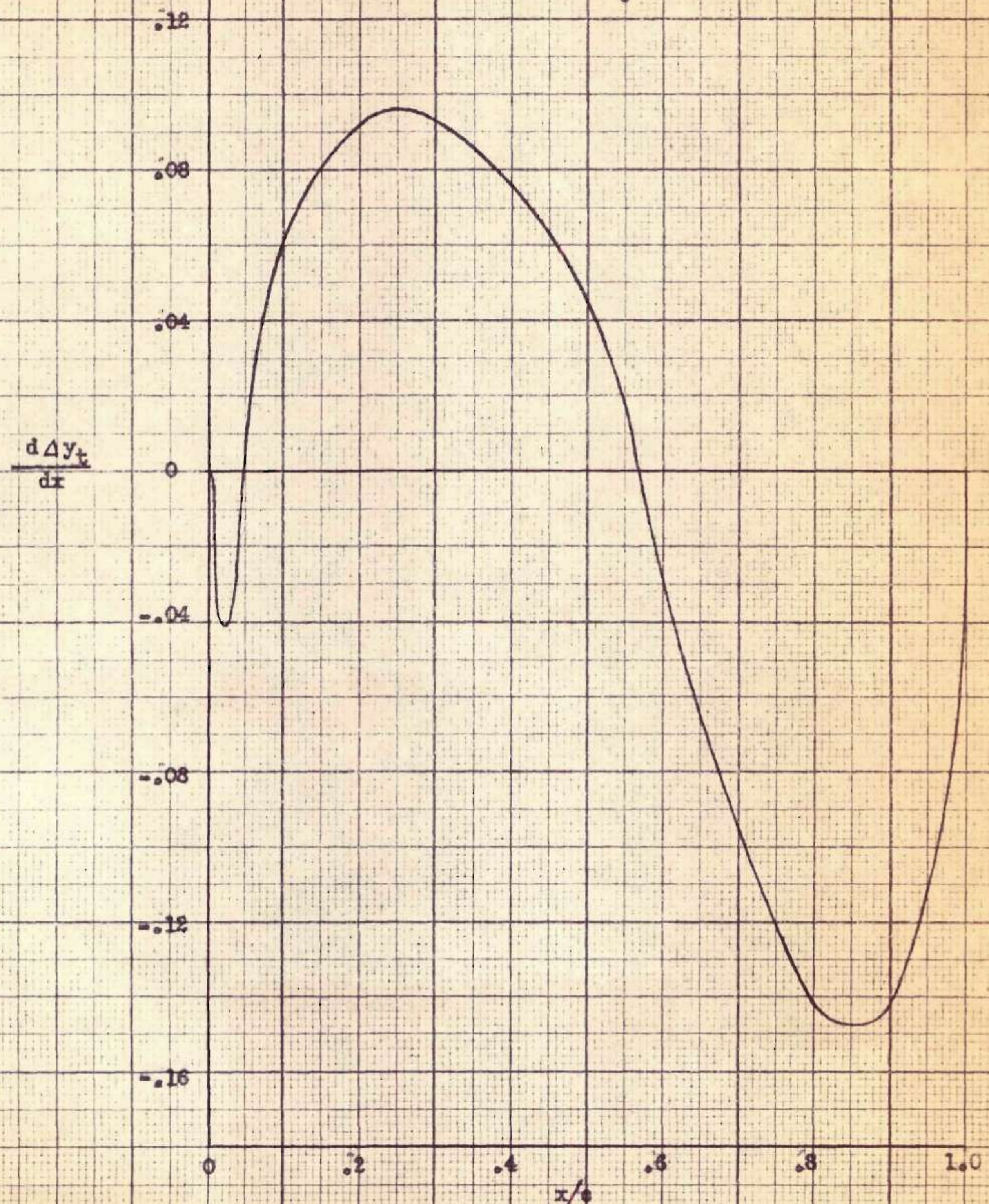

FIGURE 5

THE BASE PROFILE

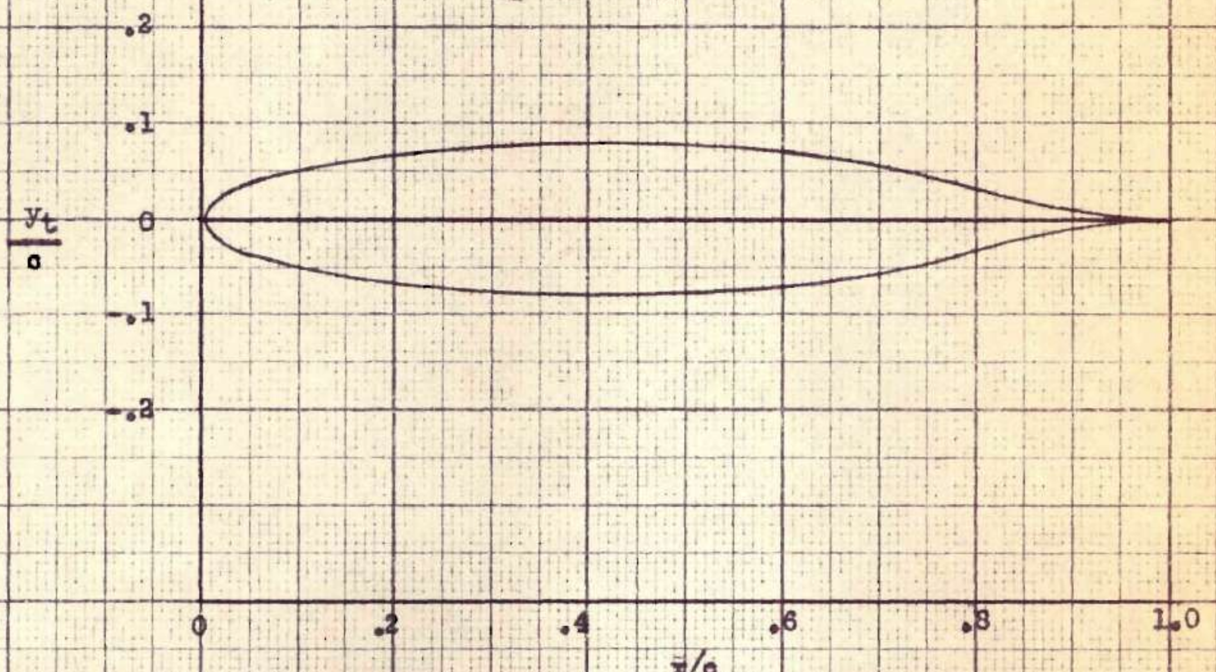

FIGURE 6

CORRECTED BASE PROFILE DISTRIBUTION. FINAL UPPER AND LOWER SURFACE VELOCITY DISTRIBUTIONS

$C_l = 0.21$

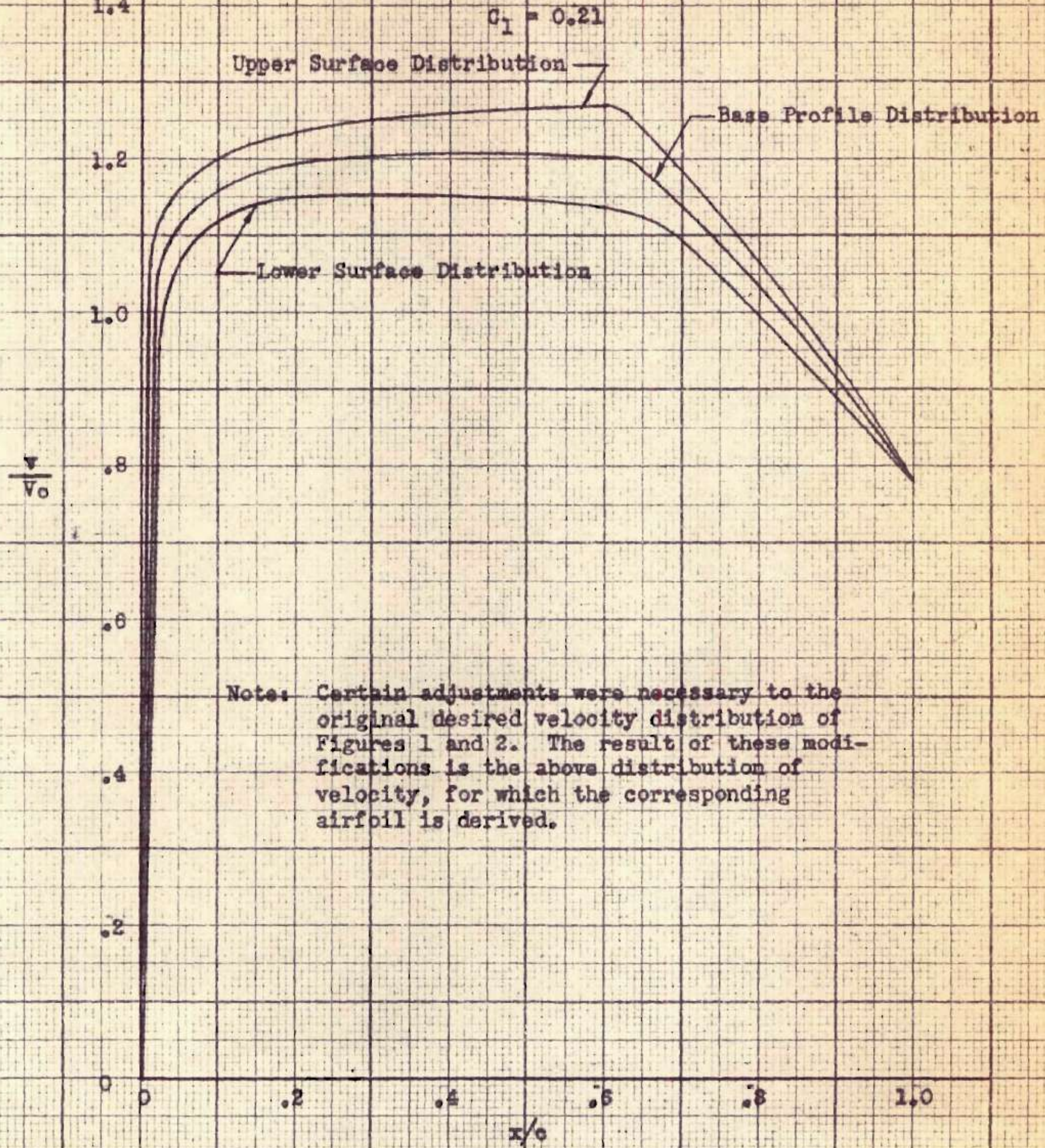

FIGURE 7

BASIC PRESSURE DISTRIBUTION FOR ZERO PROFILE THICKNESS VERSUS θ

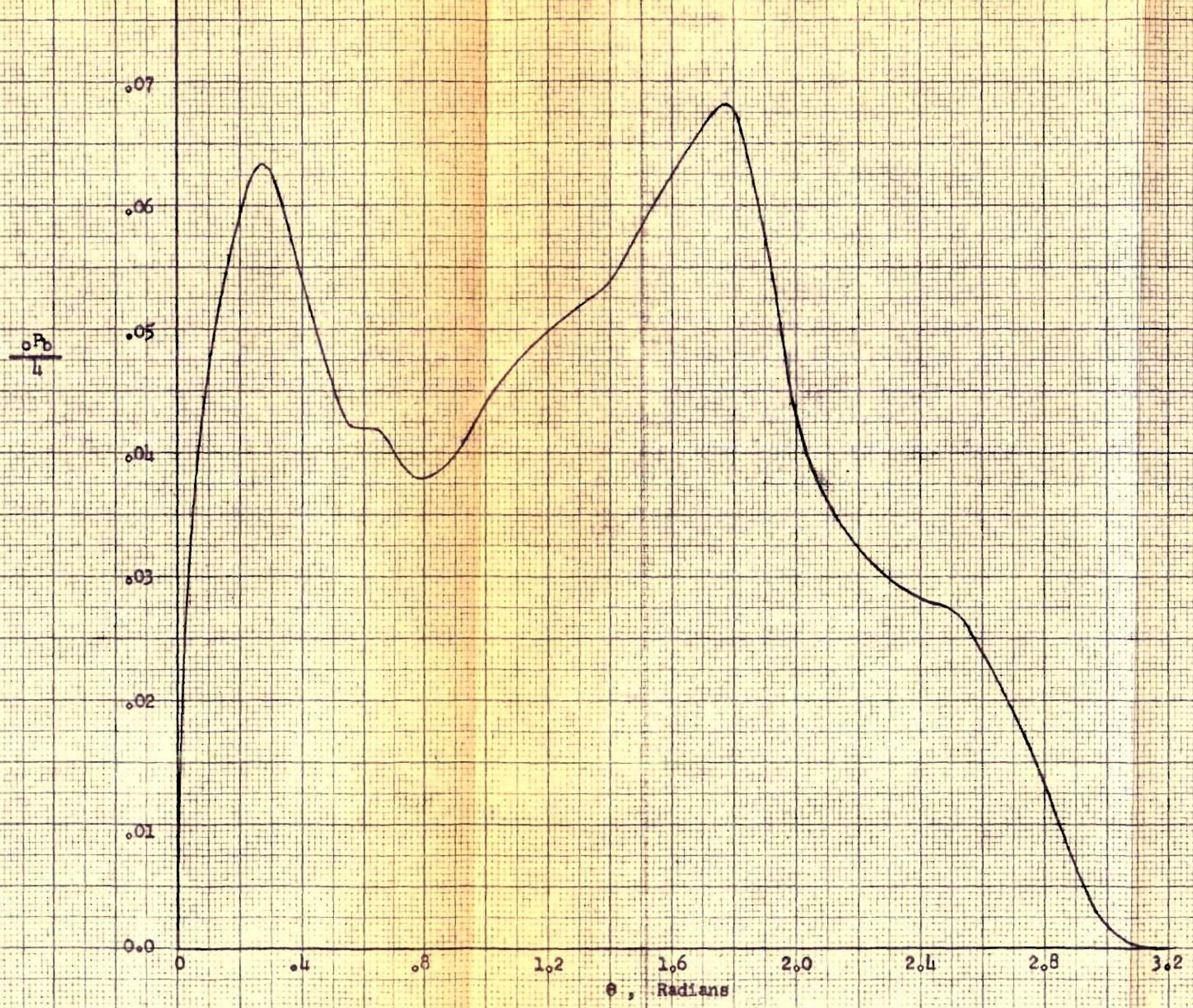

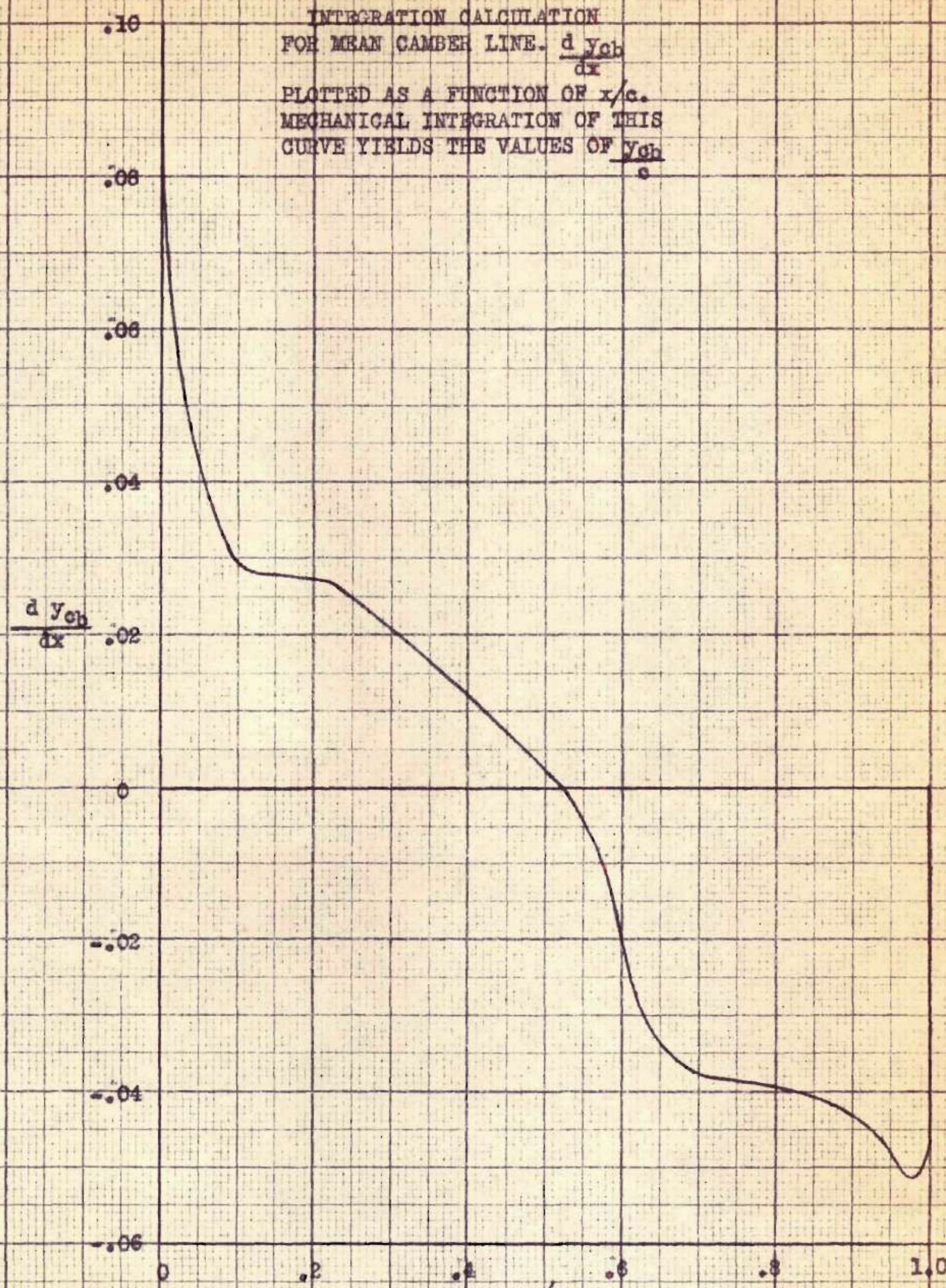

FIGURE 8

INTEGRATION CALCULATION FOR MEAN CAMBER LINE. $\frac{d\,y_{cb}}{dx}$ PLOTTED AS A FUNCTION OF x/c. MECHANICAL INTEGRATION OF THIS CURVE YIELDS THE VALUES OF $\frac{y_{cb}}{c}$

FIGURE 9

THE MEAN CAMBER LINE

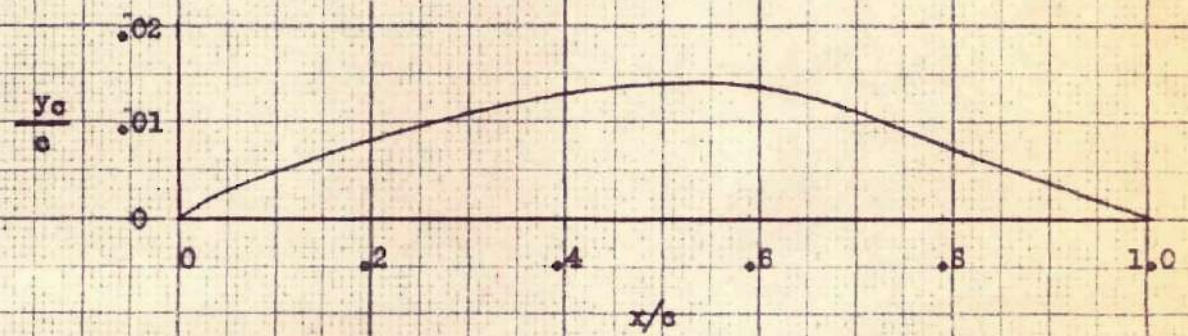

FIGURE 10

CALCULATED AIRFOIL CORRE-
ESPONDING TO THE DESIRED
VELOCITY DISTRIBUTION DE-
FINED IN FIGURE 6, AND THE
NACA 66(215)-216 AIRFOIL.

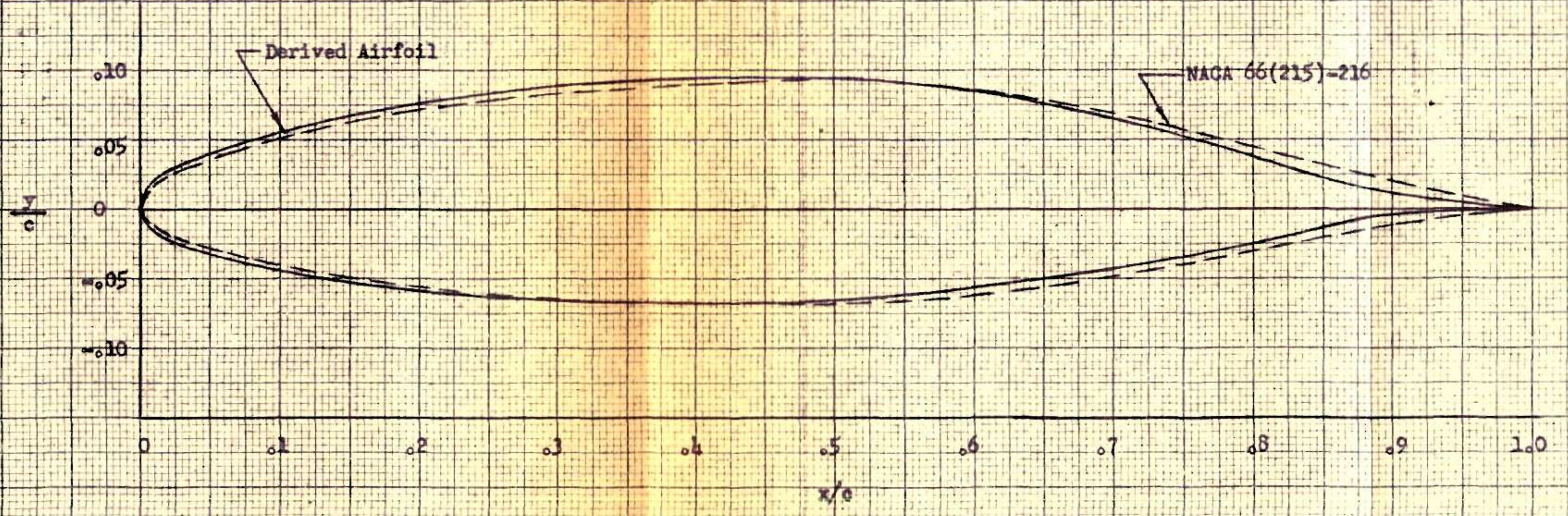

FIGURE 11

ACTUAL VELOCITY DISTRIBUTION OBTAINED FROM WIND TUNNEL TESTS OF MODEL OF THE CALCULATED AIRFOIL; COMPARISON WITH THE DESIRED VELOCITY DISTRIBUTION

$C_l = 0.21$

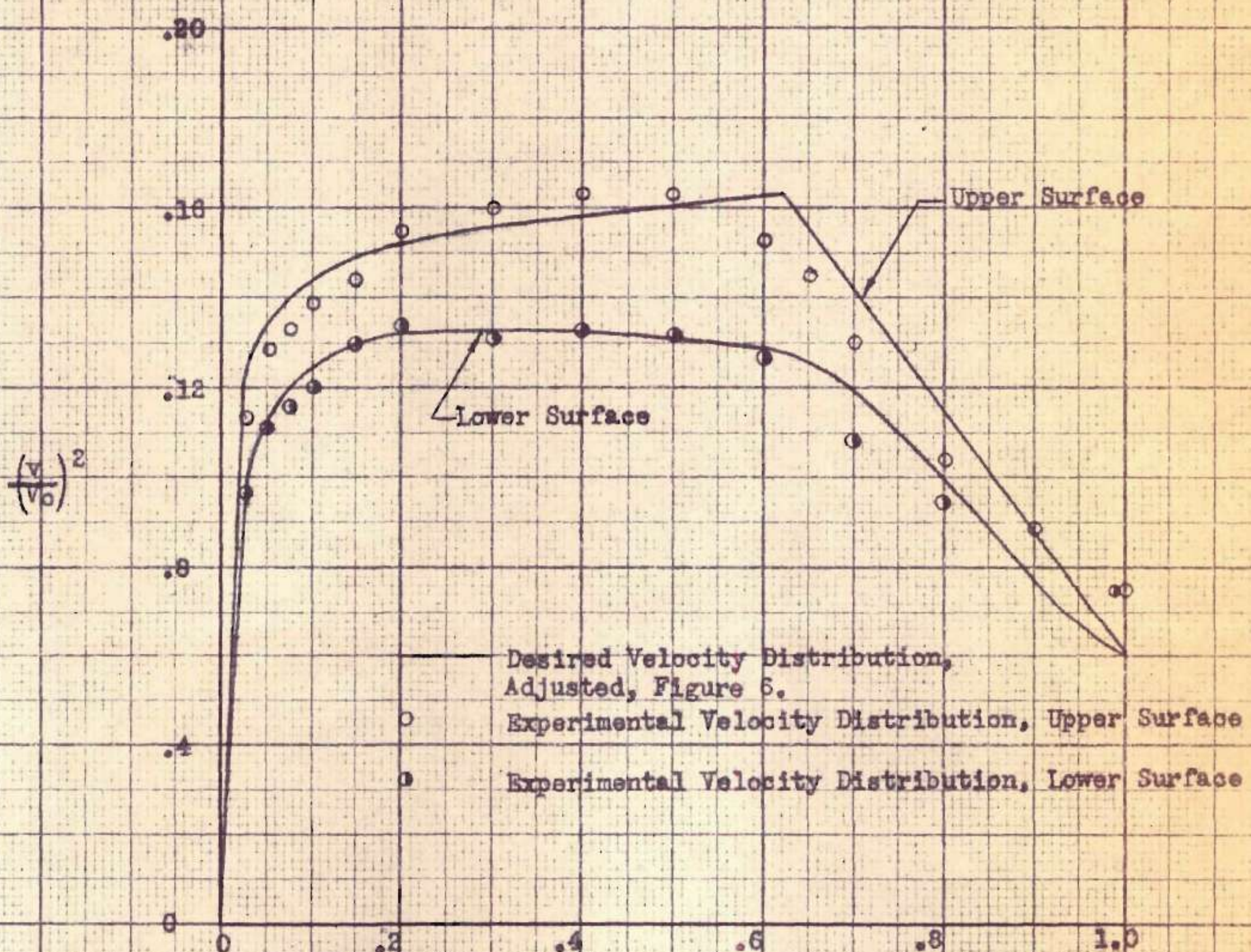

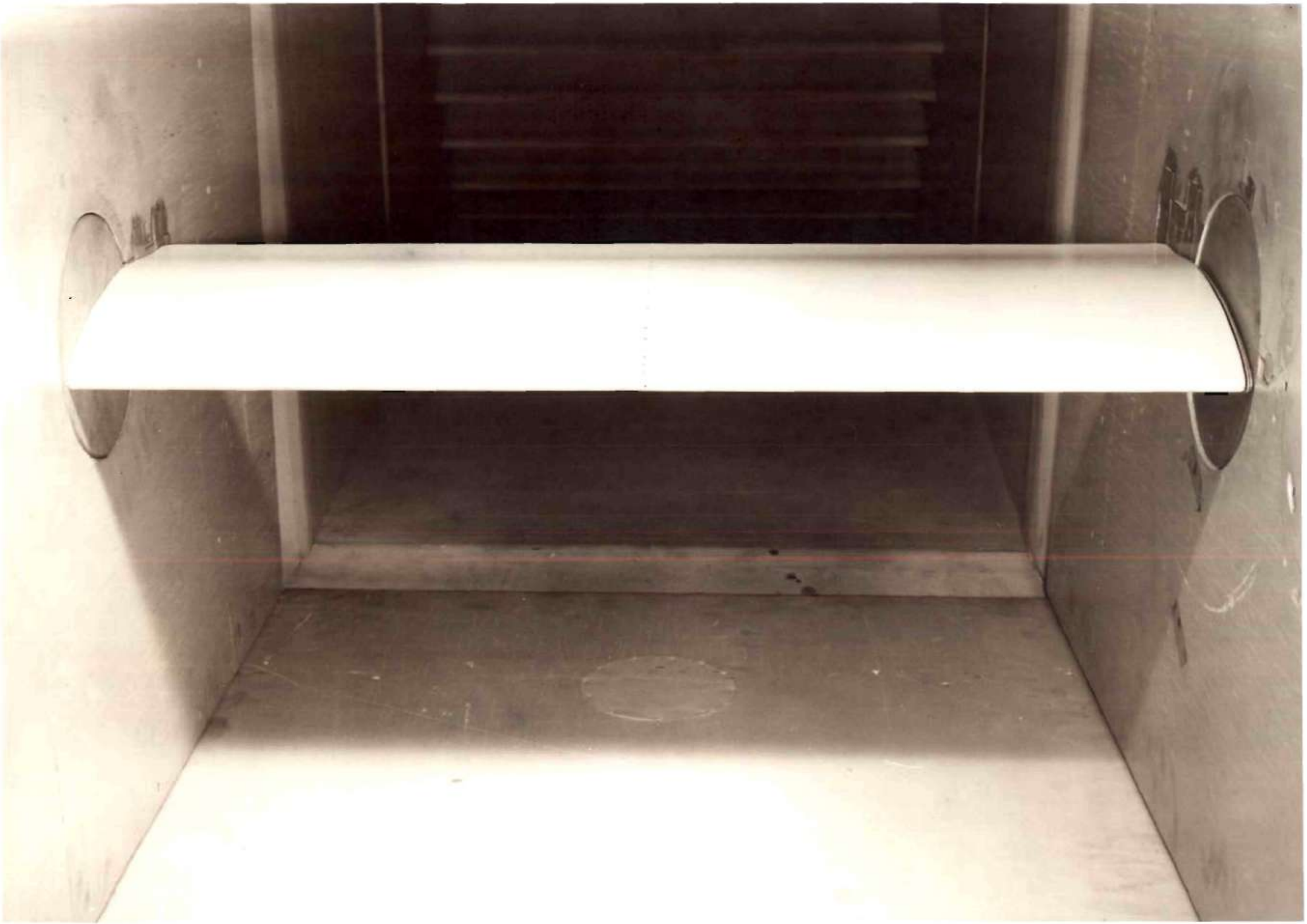

FIGURE 12. AIRFOIL MODEL IN TUNNEL TEST SECTION

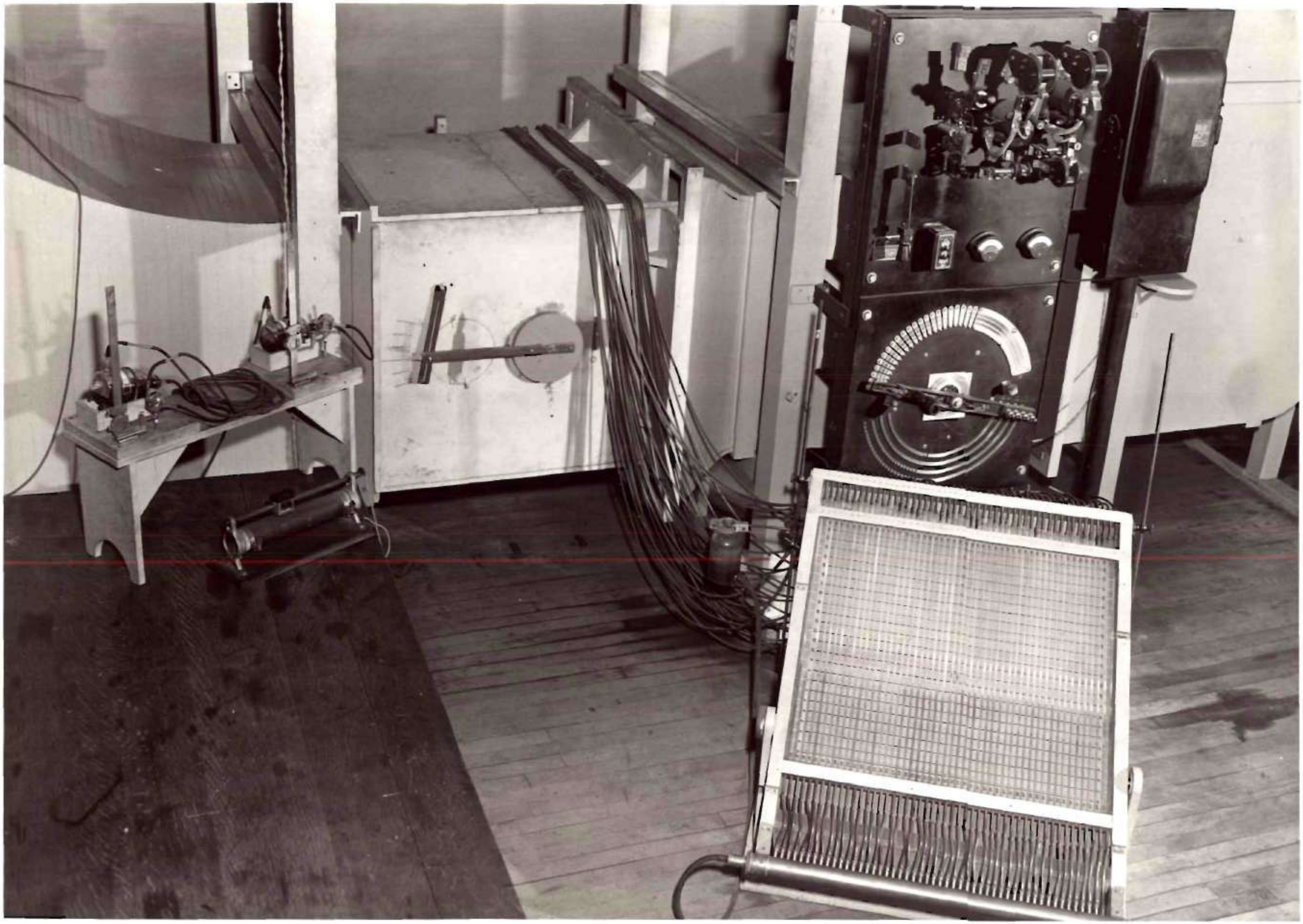

FIGURE 13. TUNNEL TEST SECTION, CONTROL PANEL, AND MANOMETERS

APPENDIX III

METHOD OF NUMERICAL INTEGRATION

METHOD OF NUMERICAL INTEGRATION

A numerical evaluation of the integral $E = \frac{1}{2\pi}\int_0^{2\pi} F \operatorname{Cot}\left(\frac{\theta-\theta_0}{2}\right) d\theta$ is given in the appendix of Reference (4). A "20-point" solution is

$$E = a_o\left(\frac{dF}{d\theta}\right)_o + a_1(F_1 - F_{-1}) + a_2(F_2 - F_{-2}) + \dots + a_9(F_9 - F_{-9})$$

where F_1 is the value of F at $\theta_o + \frac{\pi}{10}$, and F_n is the value of F at $\theta_o + \frac{n\pi}{10}$. Values of n are: n = 1, -1, 2, -2, 3, -3, . . . 9, -9.

$\left(\frac{dF}{d\theta}\right)_o$ is the value of $\frac{dF}{d\theta}$ at $\theta = \theta_o$, and the coefficients are:

$a_o = 0.1000$, $a_1 = 0.3473$, $a_2 = 0.1572$, $a_3 = 0.0996$, $a_4 = 0.0691$,
$a_5 = 0.0503$, $a_6 = 0.0366$, $a_7 = 0.0281$, $a_8 = 0.0163$, $a_9 = 0.0080$.

The value of $\frac{d\Delta y_t}{dx}$ for $\theta_o = \frac{5\pi}{10}$ given in Table III in the calculation of the base profile ordinates, for example, is obtained in the following cyclic form:

$$\begin{aligned}\frac{d\Delta y_t}{dx} = {} & 0.1000(.1952) + 0.3473(.139 - .052) + 0.1572(.056 - .009) \\ & + 0.0996(-.036 - .065) + 0.0691(-.111 - .076) + 0.0503(-.135 - 0) \\ & + 0.0366(-.111 - .076) + 0.0281(-.036 - .065) + 0.0163(.056 - .009) \\ & + 0.0080(.139 - .052) = 0.04622\end{aligned}$$

A more accurate "40-point" solution is

$E = b_o\left(\frac{dF}{d\theta}\right)_o + b_1(F_1 - F_{-1}) + b_2(F_2 - F_{-2}) + \dots + b_{19}(F_{19} - F_{-19})$ where now F_1 is the value of F at $\theta_o + \frac{\pi}{20}$, and F_n is the value of F at $\theta_o + \frac{n\pi}{20}$. The values of n are: n = 1, -1, 2, -2, 3, -3, . . . 19, -19.

$\left(\frac{dF}{d\theta}\right)_o$ is the value of $-\frac{dF}{d\theta}$ at $\theta = \theta_o$, and the coefficients are given by:

$b_o = 0.05000$, $b_1 = 0.34906$, $b_2 = 0.16129$, $b_3 = 0.10514$, $b_4 = 0.07735$,
$b_5 = 0.06057$, $b_6 = 0.04918$, $b_7 = 0.04087$, $b_8 = 0.03444$, $b_9 = 0.02929$,
$b_{10} = 0.02503$, $b_{11} = 0.02139$, $b_{12} = 0.01819$, $b_{13} = 0.01532$,
$b_{14} = 0.01273$, $b_{15} = 0.01036$, $b_{16} = 0.00814$, $b_{17} = 0.00599$,
$b_{18} = 0.00395$, $b_{19} = 0.00197$.

The "40-point" solution need be employed only when the function F changes more or less abruptly with x/c.

APPENDIX IV

CALCULATION OF REYNOLDS NUMBER OF AIRFOIL MODEL IN WIND TUNNEL TEST

CALCULATION OF REYNOLDS NUMBER OF

AIRFOIL MODEL IN WIND TUNNEL TEST

1. Atmospheric conditions: $T = 84^{\circ}F.$; $p = 28.90$ inches of mercury

2. Static pressure in test section = 2.57 centimeters of alcohol when the dynamic pressure $q = 10.03$ centimeters of alcohol. Specific gravity of alcohol = .808.

3. Determination of q in units #/ft^2

$$q = \frac{10.03 \text{ cm. alcohol} \quad \text{ft} \quad (.808)(62.4)\#}{30.5 \text{ cm.} \quad \text{ft}^3 \text{ alcohol}} = 16.58 \ \#/\text{ft}^2$$

4. Calculation of corrected density

$$\rho = \rho_o(p/p_o)(t_o/t) = .002378 \left(\frac{28.90}{29.92}\right)\left(\frac{520}{544}\right) = .002195 \text{ slugs/ft}^3$$

5. Calculation of indicated and true velocities

$$V_i^2 = \frac{2q}{\rho} = \frac{2(16.58)\# \ \text{ft}^4}{\text{ft}^2 \quad .002378\# \sec^2} = 13{,}940 \text{ ft}^2/\sec^2$$

$V_i = 118$ ft/sec = 80.5 mph.

$$V_t = V_i/\sigma^{1/2} = \frac{V_i}{\left(\frac{\rho}{\rho_o}\right)^{1/2}} = \frac{118}{\sqrt{\frac{.002195}{.002378}}} = 122.6 \text{ ft/sec} = 83.6\text{mph}$$

6. Determination of corrected viscosity

$\mu = (340.8 + 0.548 \times {}^{\circ}F)\cdot 10^{-9}$ from Reference (7)

$\mu = (340.8 + 0.548 \times 84)\cdot 10^{-9} = 386.9 \ 10^{-9} \ \#\text{sec/ft}^2$

7. Calculation of Wind Tunnel Reynolds Number

$$R.N. = \frac{\rho V c}{\mu} = \frac{.002195\#\sec^2 \quad 122.6\,[\text{ft}] \quad (\text{ft}^2) \quad 10/12 \text{ ft}}{\text{ft}^4 \quad (\#\sec) \quad 386.9 \quad [\sec]\, 10^{-9}} = 579{,}000$$

8. Determination of Effective Reynolds Number

$R.N._e$ = Turbulence Factor × Tunnel Reynolds Number; where T.F. = 1.375

$R.N._e = 1.375 \times 579{,}000 = 797{,}000$